SYNTHESES OF BENZOTRIAZOLE BEARING DONOR ACCEPTOR TYPE RANDOM COPOLYMERS FOR FULL VISIBLE LIGHT ABSORPTION

A THESIS SUBMITTED TO
THE GRADUATE SCHOOL OF NATURAL AND APPLIED SCIENCES
OF
MIDDLE EAST TECHNICAL UNIVERSITY

BY

GÖZDE ÖKTEM

IN PARTIAL FULFILLMENT OF THE REQUIREMENTS
FOR
THE DEGREE OF MASTER OF SCIENCE
IN
CHEMISTRY

SEPTEMBER 2011

Approval of the thesis:

SYNTHESES OF BENZOTRIAZOLE BEARING DONOR ACCEPTOR TYPE RANDOM COPOLYMERS FOR FULL VISIBLE LIGHT ABSORPTION

submitted by **GÖZDE ÖKTEM** in partial fulfillment of the requirements for the degree of **Master of Science in Chemistry Department, Middle East Technical University** by,

Prof. Dr. Canan Özgen
Dean, Graduate School of **Natural and Applied Sciences** _____

Prof. Dr. İlker Özkan
Head of Department, **Chemistry** _____

Prof. Dr. Levent Toppare
Supervisor, **Chemistry Dept., METU** _____

Examining Committee Members:

Assoc. Prof. Dr. Yasemin Arslan Udum
Institute of Science and Technology
Dept. of Adv. Tech., Gazi University _____

Prof. Dr. Levent Toppare
Chemistry Dept., METU _____

Assist. Prof. Dr. Ali Çırpan
Chemistry Dept., METU _____

Assist. Prof. Dr. İrem Erel
Chemistry Dept., METU _____

Assist. Prof. Dr. Ertuğrul Şahmetlioğlu
Chemistry Dept., Niğde University _____

Date: 05.09.2011

I hereby declare that all information in this document has been obtained and presented in accordance with academic rules and ethical conduct. I also declare that, as required by these rules and conduct, I have fully cited and referenced all material and results that are not original to this work.

Name, Last name: GÖZDE ÖKTEM

Signature:

ABSTRACT

SYNTHESES OF BENZOTRIAZOLE BEARING DONOR ACCEPTOR TYPE RANDOM COPOLYMERS FOR FULL VISIBLE LIGHT ABSORPTION

Öktem, Gözde
M. Sc., Department of Chemistry
Supervisor: Prof. Dr. Levent Toppare

September 2011, 80 pages

The synthesis and preliminary optoelectronic properties of a series of donor-acceptor (DA) type polymers differing by the acceptor units in the polymer backbone were investigated. Polymers CoP1, CoP2 and CoP3 were designed to yield alternating DA segments with randomly distributed different acceptor units along polymer backbone. The combination of neutral state red colored and neutral state green colored materials resulted in different neutral state colors with respect to their additional acceptor unit. 5,8-Dibromo-2,3-bis(4-*tert*-butylphenyl) quinoxaline, 5,8-dibromo-2,3-di(thiophen-2-yl)quinoxaline and 4,7-dibromobenzo[c][1,2,5]selenadiazole units were perceived as additional acceptor units and these constituents were combined with the 4,7-dibromo-2-dodecyl-2H-benzo[d][1,2,3]triazole unit and the 2,5-bis(tributylstannyl)thiophene moiety via Stille coupling. The resultant donor acceptor type random copolymers indicated that possessing 5,8-dibromo-2,3-di(thiophen-2-yl)quinoxaline as an extra electron deficient with 4,7-dibromo-2-dodecyl-2H-benzo[d][1,2,3]triazole unit on the same polymer backbone originated a neutral state black colored copolymer along with spanning the entire visible spectrum.

Keywords: Benzotriazole, Donor-Acceptor Random Copolymers, Neutral State Black Copolymers, Quinoxaline, Stille Coupling.

öz

GÖRÜNÜR BÖLGE IŞIĞININ TAM ABSORPLANMASI İÇİN BENZOTRİAZOL İÇEREN DONÖR AKSEPTÖR TİPİ RASTGELE KOPOLİMERLERİN SENTEZİ

Öktem, Gözde
Yüksek Lisans, Kimya Bölümü
Tez Yöneticisi: Prof. Dr. Levent Toppare

Eylül 2011, 80 sayfa

Polimer zinciri üzerinde akseptör ünitelerini değiştirerek sentezlenen bir seri donör akseptör (DA) tipi polimerlerin ilk optoelektronik özellikleri incelenmiştir. CoP1, CoP2 ve CoP3 olarak isimlendirilen polimerler, polimer zinciri boyunca rastgele dağılmış değişik akseptör üniteleriyle alternatif DA parçaları vermeleri için tasarlanmıştır. Eklenilen akseptör ünitelerine göre, nötr hali kırmızı ve yeşil renk olan malzemelerin birleşimi nötr hallerinde oluşan farklı renklerle sonuçlanmıştır. 5,8-Dibromo-2,3-bis(4-*tert*-butilfenil)kinokzalin, 5,8-dibromo-2,3-di(tiyofen-2-il)kinokzalin and 4,7-dibromobenzo[c][1,2,5]selenadiazol üniteleri fazladan eklenen ünitelerdir ve bu öğeler 4,7-dibromo-2-dodesil-2H-benzo[d][1,2,3]triazol bileşeni ve 2,5-bis (tributilstannil) tiyofen bileşeniyle Stille reaksiyonu yoluyla birleştirilmiştir. Sonuçta elde edilen donör akseptör tipi polimerlerden fazladan elektronca fakir bileşen olarak 5,8-dibromo-2,3-di(tiyofen-2-il)kinokzalin'e sahip olan polimerde, aynı polimer zinciri boyunca 4,7-dibromo-2-dodesil-2H-benzo[d][1,2,3]triazol ile alternatif ilerlemeleri ve görünür bölgeyi tamamen absorplaması dolayısıyla bu polimeri nötr halinde siyah renkli yapmıştır.

Anahtar Kelimeler: Benzotriazol, Donör-Akseptör Rastgele Kopolimerler, Siyah Kopolimer, Kinokzalin, Stille Reaksiyonu.

To My Precious Family

ACKNOWLEDGMENTS

First and foremost, I want to express my sincere gratitude to my supervisor Prof. Dr. Levent Toppare for his expertise, diligent guidance, and endless patience, enthusiasm in science and valuable suggestions about all steps of life. It has ben an honor for me to be his graduate student in this considerable part of my life.

I am grateful to Abidin Balan and Simge Tarkuç for their patience and trust besides their sincerity. I owe them my eternal gratitude about their contributions to my organic synthesis knowledge.

I would like to express my deepest gratitude to my classy friends Gönül, Hava, Fulya and Doğukan for their invaluable support, kind friendship and making lab life more fun. I want to thank Yasemin Udum, Başak and Naime for the scientific cooperation besides irreplaceable coffee breaks. I also thank to all of my lab buddies who helped me in many ways, in Toppare Research Group.

A very special thanks goes out to my "oldies but goldies" friends; Deniz, Döndü, Engin, Fulya, Hakan, İpek, Seda, Şenz, Utku for this long standing valuable friendship besides their inspiring suggestions and enjoyable memories.

Finally, words alone cannot express the thanks I owe to my dear family who insistently supported me in any respect, throughout my life. It is tremendous to feel your love always by my side.

TABLE OF CONTENTS

LIST OF TABLES

TABLES

LIST OF FIGURES

FIGURES

ABBREVIATIONS

ACN	Acetonitrile
BIm	Benzimidazole
BSe	Benzoselenadiazole
BTd	Benzothiadiazole
BTz	Benzotriazole
CB	Conduction Band
CP	Conducting Polymer
CV	Cyclic Voltammetry
DA	Donor- Acceptor
DCM	Dichloromethane
DOTs	Dioxythiophenes
ECD	Electrochromic Device
EDOT	3,4-Ethylenedioxythiophene
E_g	Band Gap Energy
GPC	Gel Permeation Chromatography
HOMO	Highest Occupied Molecular Orbital
ITO	Indium Tin Oxide
LUMO	Lowest Unoccupied Molecular Orbital
NHE	Normal Hydrogen Electrode
NMR	Nuclear Magnetic Resonance
PAc	Polyacetylene
PBEBT	Poly(4,7-bis(2,3-dihydrothieno[3,4-b][1,4]dioxin-5-yl)-2-dodecyl-2H-benzo[1,2,3]triazole)
PCz	Polycarbazole
PDI	Polydispersity Index
PEDOP	Poly(3,4-ethylenedioxypyrrole)
PEDOT	Poly(3,4-ethylenedioxythiophene)
PF	Polyfuran
PFBT	Poly(2-dodecyl-4,7-di(furan-2-yl)-2Hbenzo[d][1,2,3]triazole)
PHTBT	Poly(4,7-bis(3-hexylthien-5-yl) 2-dodecyl-benzo[1,2, 3]triazole)
PITN	Poly(isothianaphthene)

PProDOT	Poly(propylenedioxythiophene)
PPy	Polypyrrole
PPyBT	Poly(2-dodecyl-4,7-di(1H-pyrrol-2-yl)-2H-benzo[1,2,3]triazole)
PSeBT	Poly(2-dodecyl-4,7-di(selenophen-2-yl)benzotriazole)
PTBPTQ	Poly(2,3-bis(4-tert-butylphenyl)-5,8-di(thiophen-2-yl)quinoxaline)
PTBT	Poly(2-dodecyl-4,7-di(thiophen-2-yl)-2Hbenzo[d][1,2,3]triazole)
PTh	Polythiophene
PTSA	*p*-toluene sulfonic acid
PTSeT	Poly(4,7-di-2-thienyl-2,1,3-benzoselenadiazole)
PTTBT	Poly(2-dodecyl-4,7-di(thieno[3,2-b]thiophen-2-yl)-2H-benzo[d] [1,2,3]triazole)
PTTQ	Poly(2,3,5,8-tetra(thiophen-2-yl)quinoxaline)
RGB	Red- Green-Blue
$TBAPF_6$	Tetrabutylammonium hexafluorophosphate
THF	Tetrahydrofuran
VB	Valence Band

CHAPTER 1

INTRODUCTION

1.1 Π Conjugated Polymers

Conjugated polymers (CPs) are a fundamental research subject both in academia and industry. Many different types and derivatives of CPs have been successfully prepared over the decades and their potential as advanced materials has been investigated in several optoelectronic applications [1-2]. The history of conjugated polymers started with electrolytic oxidation of aniline in dilute sulfuric acid by Letheby in 1862 [3]. Even history started as far back as 1862, the master developments in conjugated polymers took form at the end of 1970s. The enhancement in the conductivity of polyacetylene (PAc) silvery thin film via exposure to halogens was officially opened a new era in 1977. Shirakawa *et al.* reported that the charge transfer containing oxidative coupling of the trans isomer of PAc produces a thermodynamically stable polymer at room temperature. With strong electron deficient materials such as iodine and bromine a vast increase in the conductivity of PAc can be achieved[4]. This magnific contribution to the scientific world was awarded with the Nobel Prize in Chemistry given to Hideki Shirakawa, Alan Heeger and Alan MacDiarmid in 2000. By this tremendous breakthrough work, a new field combining heterocyclic chemistry with conductivity allowed the emergence of conducting polymers [5]. All the intention for this area focuses on creating air stable and processable new materials as conductive as PAc, the archetype of conducting polymers. That leads researchers study on aromatic and heterocyclic compounds and allows emerging of tons of conducting materials having these heterocyclics along the polymer chain.

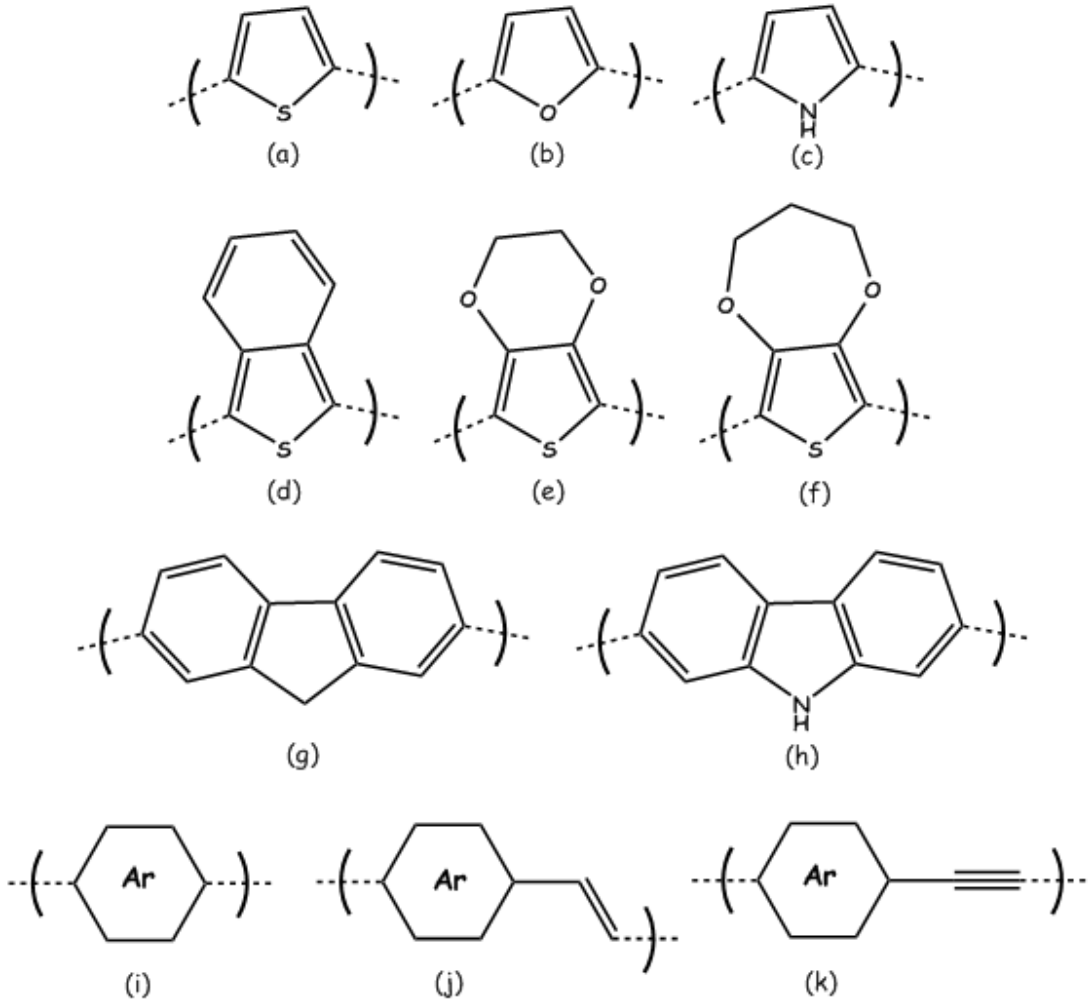

Figure 1. 1 Chemical structures of some common π- conjugated polymers. (a) polythiophenes (PTh), (b) polyfuran (PF), (c) polypyrroles (PPy), (d) poly(isothianaphthene) (PITN),(e) poly(ethylenedioxythiophene) (PEDOT), (f) poly(propylenedioxythiophene) (PProDOT), (g) polyfluorenes , (h) polycarbazole (PCz), (i) poly(arylene)s, (j) poly(arylene-vinylene)s, (k) poly(arylene-ethynylene)s

1.1.1 From Conjugated to Conducting Polymers: Doping Process

Conjugated polymers (CPs) are the new generations of polymers containing π-electron backbone responsible for their conducting properties. The movement of positive or negative charge carriers along the conjugated polymer backbone undertakes the key role in the mechanism of conductivity. These charge carriers are generated upon oxidation and reduction processes; in the oxidation process, the formation of positively (p type doping) charged carriers occurs, while for the reduction process, negatively (n type doping) charged carriers are formed [6-7].
In detail, the removal of an electron from the "valence band" during oxidation generates partial delocalization by leaving a radical cation behind on the conjugated polymer backbone. As a result of the generated positive charge delocalization, the withdrawal of electrons from the lone pairs of the heteroatoms occurs leading the evolution of quinoidal structure (Figure 1.2) [8]. This delocalization gives rise to the formation of polaron bands lying between HOMO and LUMO levels of the conjugated polymer.

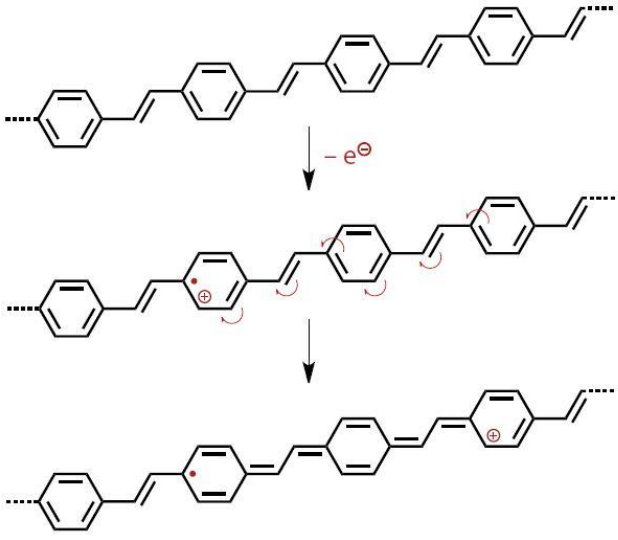

Figure 1.2 The partial delocalization of positive charge carriers on the polymer backbone leading the polaron bands

In concurrence with the formation of polaron bands, the absorbance of the polymer backbone possessing partial delocalization is red shifted compare to the neutral form. Afterwards, the removal of the second electron originates radical dication on the same backbone, at this time, served as bipolaron bands (Figure 1.3). By means of the movement of polarons and bipolarons along the polymer chain upon applied potential, the conductivity of conjugated polymers is extended.

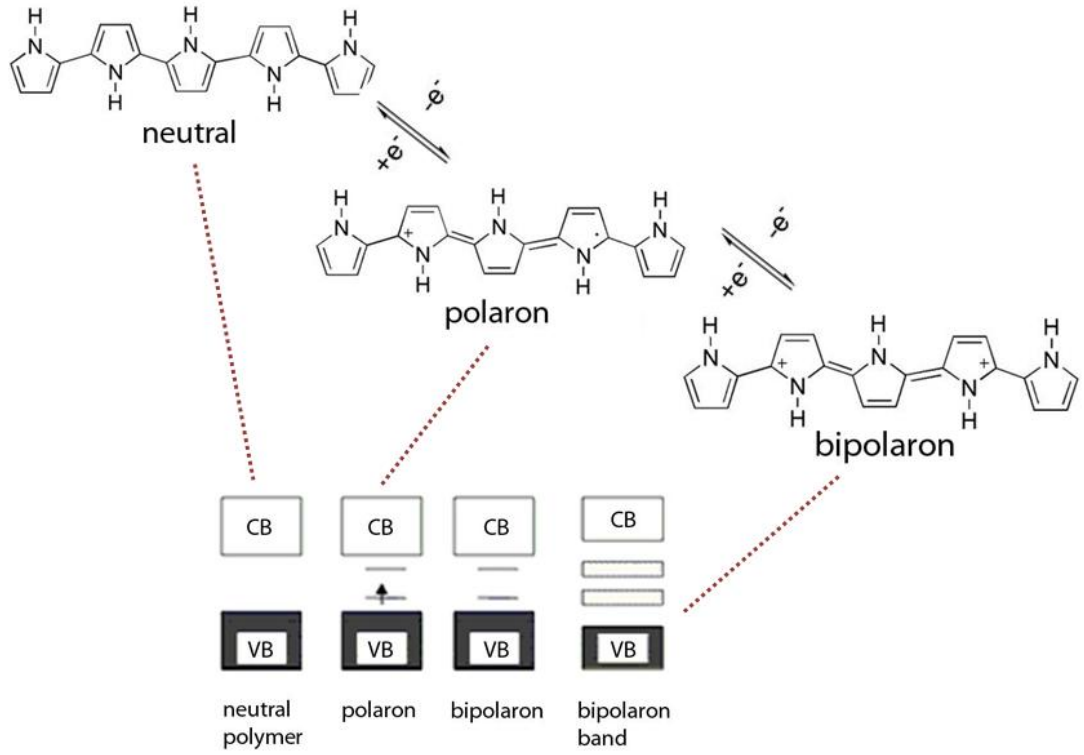

Figure 1.3 Charge carries in PPy and its corresponding energy bands.

1.1.2 Evolution of the Band gap

Conductors, semiconductors and insulators are regarded as three classes of the materials in terms of conductivity at room temperature. For the conducting polymeric materials which are semiconductors, the band theory is utilized to

express the electrical characteristics of these semiconductors. The band gap is the difference between the highest occupied electronic levels generating valence band and the lowest unoccupied electronic levels generating the conduction band [9]. The band gap of conducting polymers lies between conductors possessing a zero band gap due to the overlapping in conduction and valence bands, and insulators that electron transitions does not occur in the case of large band gap among valence and conduction band. By means of the motion of the charge carriers along the polymer chain, the generation of polaron and bipolaron discrete levels referred as bands leads to the metallic conductivity in conducting polymers.

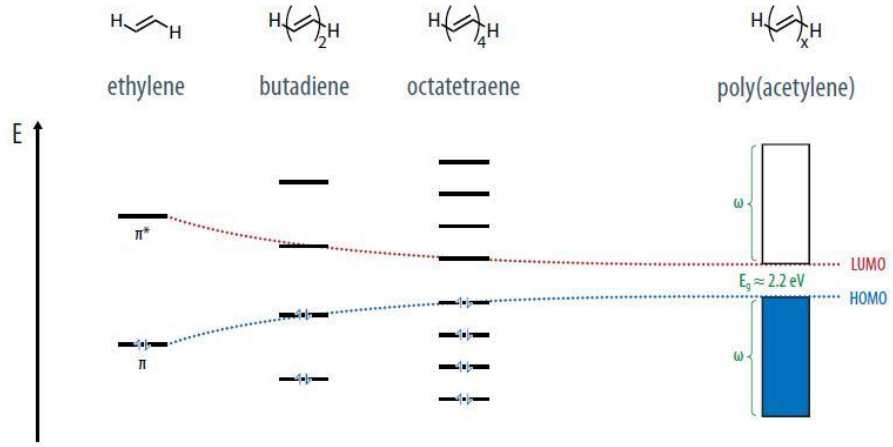

Figure 1.4 The formation of band structure as conjugation increases

π- conjugated polymers comprise carbon atoms having sp^2p_z hybridization in their backbones, meaning that each of the carbon atoms in the sp^2 form has three identical σ bonds, while "p_z" denotes the π overlapping with the neighboring p_z orbital (Figure 1.5). Due to this overlapping between the π orbitals along the polymer chain, delocalization occurs. In this manner, the "conjugation" concept is based on the alternating single and double carbon-carbon covalent bonds leading the overlap of the $2p_z$ orbital of carbon atoms [10]. This overlapping between π orbitals of the repeating units along the

polymer chain increase with the extent of conjugation length and the discrete electronic levels become bands (Figure 1.4).

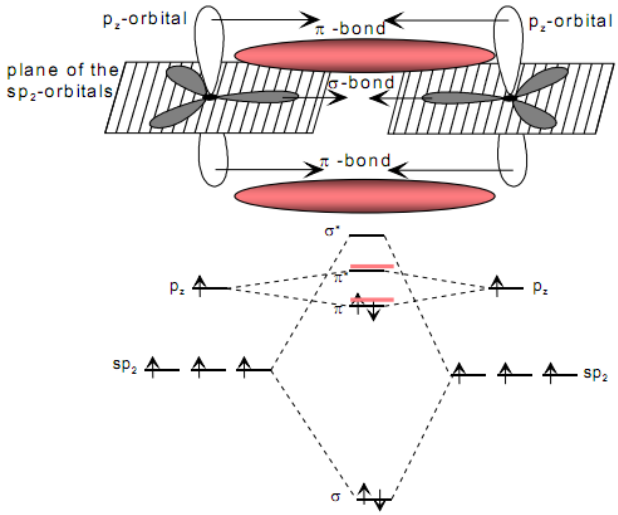

Figure 1.5 The representation of overlapping in π orbitals

The difference between valence band and conduction band which defines the electronic and optoelectronic features of the π conjugated systems can be controlled via various strategies. The structural alterations in conjugated polymers lead one to control not only the optical and electronic properties of the polymers, but also give the opportunity to create low band gap polymers. These structural alterations consist of the change in bond length of polymer, the deviation from planarity, interchain effects, inductive or mesomeric effects and the intramolecular charge transfer.

The earliest low band gap polymer is poly(isothianaphthene) (PITN), which is the combination of thiophene and more aromatic benzene, hence the band gap narrows due to the aromatic and quinoid geometries which affects the bond length of the polymer [11]. The quinoidal structure is expected to be energetically more stable due to the occurrence of the more aromatic form during delocalization. The alterations in band gap can be adjusted; via bond length alternation seen in the PITN case, the deviation from planarity of the system by creating more rigid structure, stereoregularity interchain effects,

change in inductive or mesomeric effects with insertion of electron withdrawing and donor groups on polymer backbone and finally intramolecular charge transfer provided by donor acceptor approach [12].

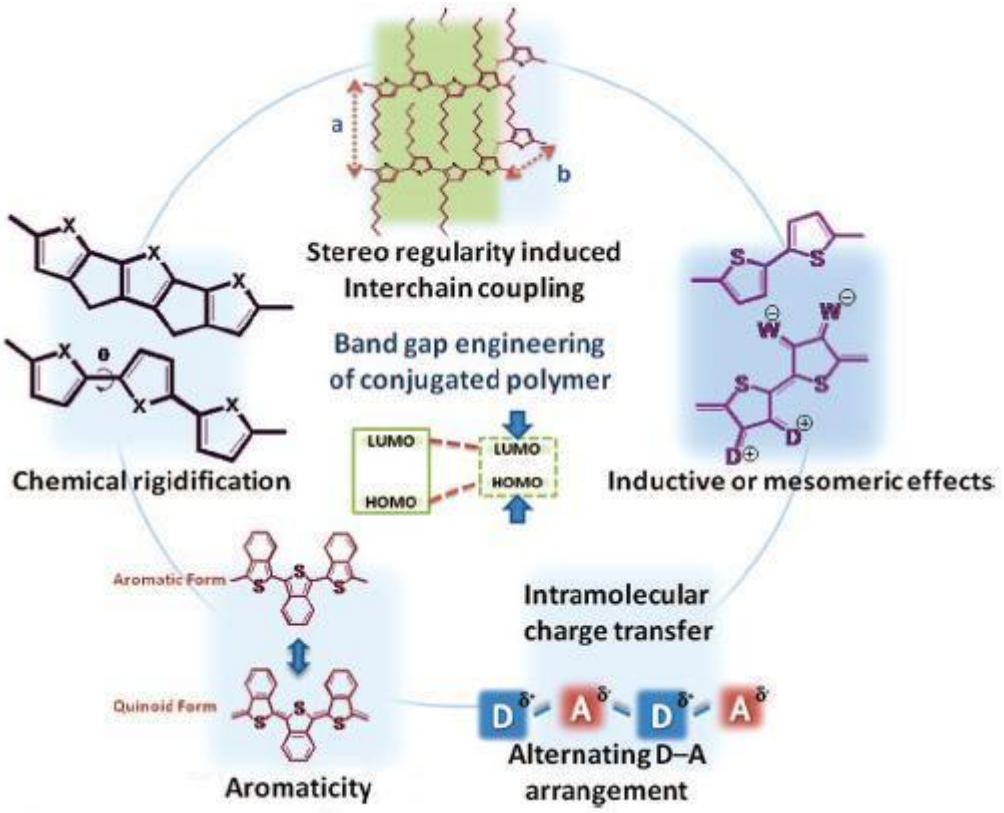

Figure 1.6 The band gap engineering strategies for conjugated polymers

1.1.3 Donor- Acceptor Theory

In order to tune the band gap and thus optical and electronic properties, structural design is the keystone. There are several methods utilized for structural modifications [13]. However, to obtain desired CPs, recent research interest have mainly focused on donor-acceptor (DA) type materials in which electron rich and electron deficient groups are both present on the backbone

[14]. Alternating donor and acceptor units bearing conjugated polymers are claimed as essential to manipulate the band gap. The donor acceptor theory is the most convenient method by means of offering tremendous facilities in the sense of synthetic pathways. These facilities allow the production of multipurpose smart materials which can be used efficiently in many different optoelectronic applications. The donor-acceptor approach is predicated on assembling an electron rich unit with high HOMO level and an electron deficient unit with low LUMO level in a new structure. In addition to the presence of strong electron donor and acceptor components, the "match" between these constituents is considerable. Reynolds *et al.* pointed this approach by means of designing polymers possessing cyanovinylene group as the electron deficient element with varied electron donor elements (Figure 1.7) [15]. In this study, the change in electron transmitting ability contributes to the effective donor acceptor match, so as to the reduction of band gap.

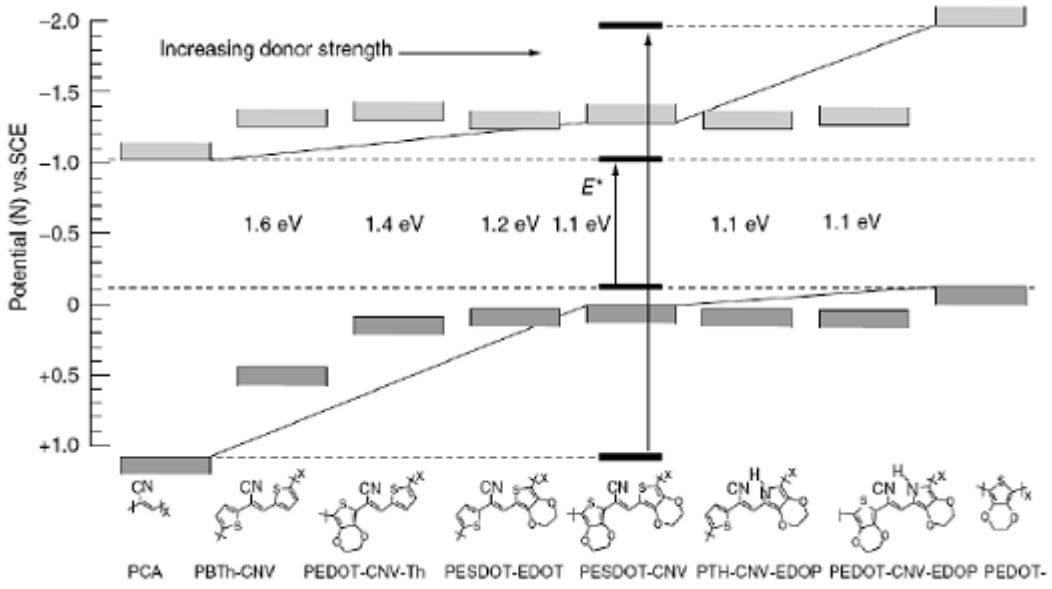

Figure 1.7 The effect of increasing donor strength on the Donor-Acceptor match and band gap

1.2 Electron Deficient Constituents

Quinoxalines are the aromatic heterocycles containing both benzene and pyrazine rings otherwise known as benzopyrazine. Owing to the imine nitrogens in the structure, quinoxalines are utilized as strong acceptor components in π conjugated polymers. Due to this benzene fused pyrazine nature enabling wide application areas, quinoxaline has attracted much attention both in photovoltaics and pharmaceuticals.

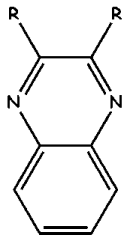

Figure 1.8 Structure of quinoxaline

Due to the distinct electrical and optical properties, the benzene fused aromatic heterocycles termed as benzazoles have been developed up to date. High electron deficient ability allows "benzazoles" to be used as "acceptor" units for the synthesis of conjugated polymers via donor acceptor approach. This high electron transporting feature originates from the presence of two electron withdrawing imine bonds (C=N) in all benzazole derivatives. Benzimidazoles (BIm), benzoselenadiazoles (BSe), benzothiadiazoles (BTd) and benzotriazoles (BTz) are the classes of benzazoles (Figure 1.9) which are the center of interest for conjugated polymer structures, nowadays. All these benzazole derivatives have distinct properties on account of diversity in polarizability between the atoms at 2 positions as seen in Figure 1.9, which also affects the electron density of the entire system. The properties relying on optical and electrochemical nature of the desired π conjugated polymers show variety due to the inequality in the characteristics based on the electronic nature between carbon, selenium, sulfur and nitrogen atoms that positioned in their 2-positions [16]. Due to the large polarizability and electrochemical amphotericity of the

selenium atom over others, benzoselenadiazole is reported as the best electron deficient unit among benzazoles [17].

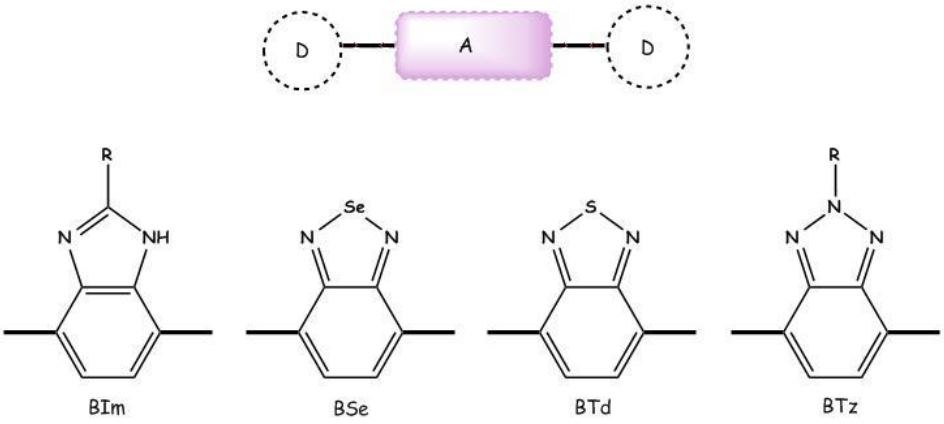

Figure 1.9 Benzazole derivatives

In literature, there are many various donor acceptor type conjugated polymers possessing benzazoles as the acceptor unit and donor units including thiophene, pyrrole, carbazole etc. due to their electron rich nature.

1.2.1 Benzotriazole based Conjugated Polymers

Benzotriazole (Btz) as a class of benzazoles, is a heteroaromatic derivative having strong electron transporting ability arising from electron withdrawing nature of imine bonds (C=N). Yamamoto *et al.* reported first Btz bearing conjugated polymers and published a study where BTz ranks first among benzazoles in terms of the electron accepting ability [18]. The first electrochemically polymerized Btz bearing conjugated polymer was designed by Toppare *et al.* in 2008 [19]. The polymer (PBEBT) is formed via the incorporation of the BTz unit well-known with its electron deficient nature with famous electron donor constituent, poly(ethylenedioxythiophene) (PEDOT). With this combination, a linearly polymerized PEDOT like structure is achieved. Actually, the electrochromic properties of PEDOT such as optical contrast, switching time etc. were enhanced by the synthesis of PBEBT. BTz constituent makes a major

contribution on not only the electrochromic properties of PEDOT, but also extends the doping ability to the ambipolar character with the help of high electron accepting ability of BTz unit. From this point of view, Btz based conjugated polymers are important due to the improvement of parent polymers in addition to the extended solubility owing to alkyl substitution on 1-nitrogen position. In consequence of the utility of BTz unit, several conjugated polymers containing BTz on the polymer backbone are synthesized. The polymer, PTBT, synthesized by the coupling of BTz and thiophene (Th) units reveals the most promising characteristics among other polymers containing BTz unit. PTBT is a major breakthrough due to its electrochromic properties including "processability" and red to transmissive switching with showing all RGB colors in addition to black color [20]. Providing these magnificent properties makes BTz a perfect candidate for donor acceptor type polymers, and the electrochromic studies are canalized to BTz containing conjugated polymers.

As a result of these studies, the electronic properties of materials are identified mainly with the donor acceptor match. For instance, electron rich nature of selenophene unit over thiophene is pointless when the BTz incorporated polymers are in question, since they have the same oxidation potential. Accordingly, the conjugated polymers should have examined as a whole, not in parts in terms of electron donating or accepting ability. From this point of view, among BTz based conjugated polymers seen in Figure 1.10, PPyBT including pyrrole incorporated benzotriazole polymer chain, is the most easily oxidized polymer with the highest electron transporting character [21]. The BTz bearing polymers are arranged in order regarding the decrease in the electron donating ability as; PPyBT [21]> PBEBT [19] > P5 [22] > PFBT [23] > PHTBT [24]- PTBT [20]- PSeBT [25] > PTTBT [23]. As regards to neutral state colors, PBEBT, PPyBT and P5 are blue, whereas all other polymers are red. On account of the presence of the polaronic absorptions of these three blue neutral states colored BTz bearing polymers at higher wavelengths, the oxidation ends up with transmissive states.

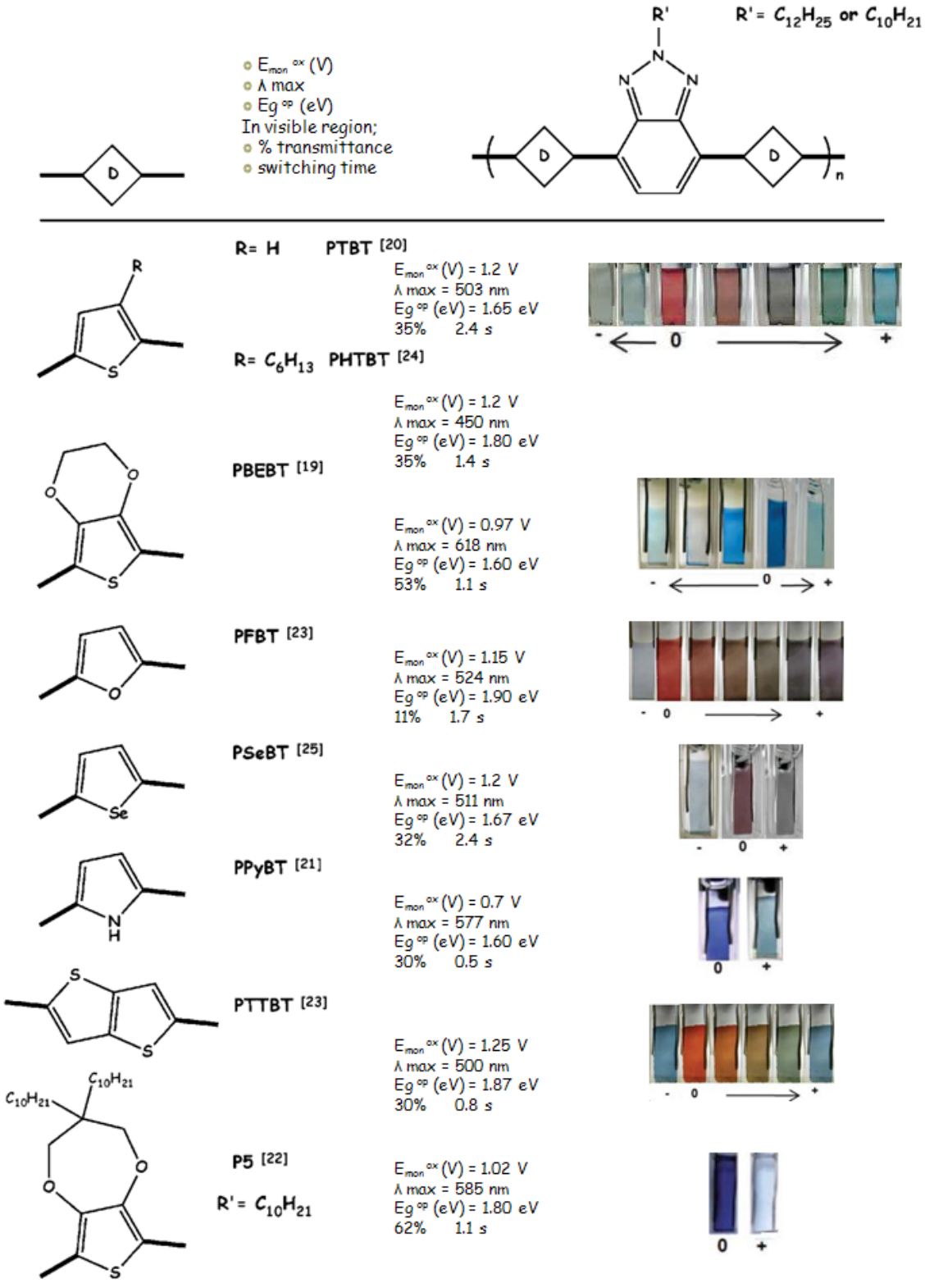

Figure 1.10 Benzotriazole bearing conjugated polymers

1.3 Electrochromism

The reversible change in color or transmission upon applied external chemical or physical stimuli is widely known as chromism. Chromism takes different titles with respect to applied stimuli; when stimulus is light, heat, potential, solvent etc., the chromism becomes photochromism, thermochromism, electrochromism and solvatochromism, respectively [26]. In electrochromism, the effect of electrochemically stimulated oxidation reduction reaction on the optical properties of the materials is examined. Upon applied potential, different electronic absorption bands are generated in the visible region as a response, while the material switching between its redox states [27]. These stimuli-responsive materials may show a variety of colors at their intermediate states, in addition to the colors at their neutral, reduced and oxidized states and they are entitled as polyelectrochromic materials [28]. The effects of the applied potential on material may not only be observed in visible region, but also in ultraviolet and infrared regions of the electromagnetic spectrum.

The electrochromic materials can be classified as metal-oxide films, molecular dyes and conducting polymers. As an electrochromic metal oxide, the most studied one is tungsten trioxide (WO_3). The electrochromism in WO_3 film basically depends on the change in color from transparent to blue via generation of W^{V} sites from W^{VI} sites upon electrochemical reduction that includes injection and ejection of metal cations (H^+, Li^+, Na^+ or K^+) and electrons according to the equation given below [29].

$$WO_3 + x(\text{Metal})^{+} + xe^{-} \rightarrow (\text{Metal})_x WO_3$$

Molecular dyes, especially viologens are a class of electrochromic materials comprising by the diquaternization of 4,4'-bipyridyl to yield 1,1'-disubstituted-4,4'-bipyridilium salts[30]. The electrochromism in viologens depends on the formation of viologens radical cations, the most colored redox state, via reductive electron transfer. While the color of the radical cation form of methyl substituted viologens is intense blue-violet color, the dication and neutral form is almost colorless.

1.3.1 Color Control in π Conjugated Polymers via Structural Modifications

While maintaining electrical conduction on the conjugated polymer backbone, partial delocalizations on the polymer chain occur via formation of the quinoid structure of the polymer. New electronic states are introduced with the change in the aromatic structure upon doping. In concurrence with the formation of polaron bands, the absorbance of the polymer backbone is red shifted compare to the neutral form. The extent of this shift relies on the band gap of the polymer. The removal of the second electron originates dications hence, bipolaron bands. Due to the mobility of polarons and bipolarons along the polymer chain upon applied potential, the conductivity of conjugated polymers is satisfied. Thus, the color of polymer in its oxidized state is determined by the energy gap between the bipolaron band and the conduction band. The structural design is the keystone to alter not only the band gap of the conducting polymers, but also their optical and electronic properties. When intending to structural design, it comprises all small changes in structure covering the conjugation length and side groups [12].

For this reason, by the introduction of some electron rich or poor groups to the polymer backbone, both band gap and color can be modulated [31]. When electron rich elements are present on the polymer backbone, the energy of valence band, HOMO of the conjugated chain increases, while the band gap of the conjugated polymer narrows. Additionally, with narrowing the energy gap, the optical absorption shifts to longer wavelengths. In the same manner, electron withdrawing groups inserted on polymer chain decrease the energy of valence band by extending the band gap thus, absorption shifts to shorter wavelengths.

Alkyl substituted polythiophenes seen in Figure 1.11, show neutral state red color and oxidized state green-gray color. When the electron rich units locate at 3,4 positions of thiophene to form PEDOT, the neutral state absorption of polymer is shifted to red region due to the increase in HOMO of the conjugated

chain, decrease in energy gap. As a result of absorption shifting to longer wavelengths, PEDOT becomes blue in its undoped form [32].

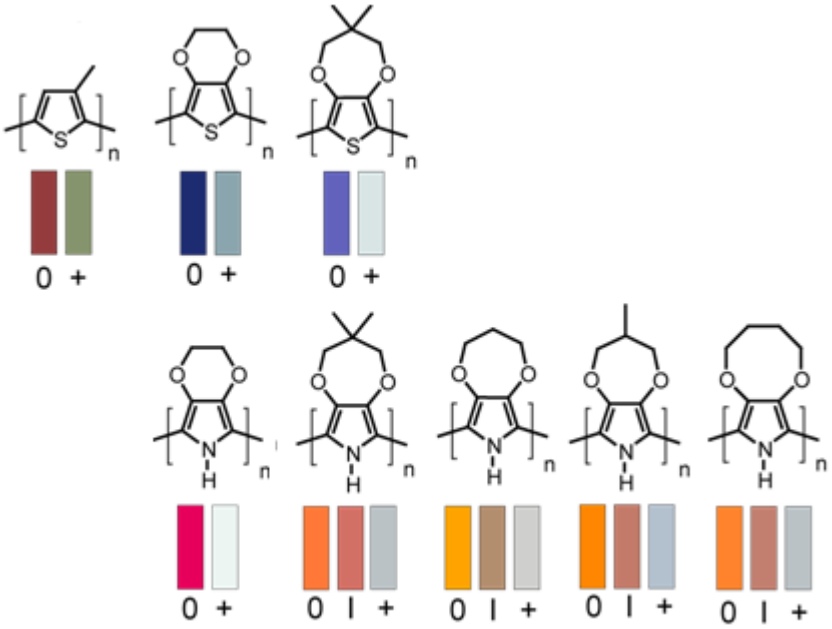

Figure 1.11 The change in neutral and oxidized state colors with small alterations in the structures of main donor units

As seen in Figure 1.12, due to the interannular rotations of single bonds between aromatic thiophene units, the angle varies the overlap of π orbitals. Conjugated polymers formed by the mono alkyl substituted thiophene units prevent the coplanarity of polymer backbone by the steric interactions and cause a decrease in the conjugation length of the polymer. As a result, the band gap increases and blue shifted emission occurs. In other words, poly(3,4-dialkylthiophenes) should have higher oxidation potentials and band gaps than mono alkyl substituted polythiophenes [33].

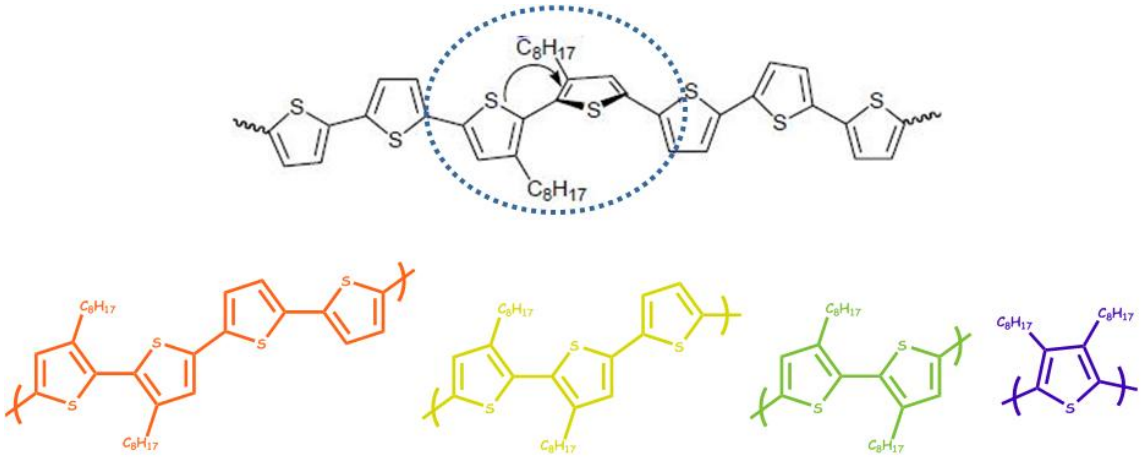

Figure 1.12 The interannular rotation of single bonds and resulted emission colors of conjugated polymers given in structure

1.3.2 The Visible Spectrum and Neutral State Colors of Polymers

The electromagnetic spectrum include the visible part in the range between 380 nm and 740 nm where human eye perceives through eye-brain coordination system. The colors are qualified by human eye with respect to the sensitivity of cone cells in the human retina to the different wavelengths of light, in other words, light is reduced to three color components by eye.When the light hits an object, the photons can be either absorbed or reflected by material and the human eye only can see colors that the surface of the object reflects. For instance, the green appearance of objects is provided by the absorption of red and blue photons and the allowance of green photons to bounce back.

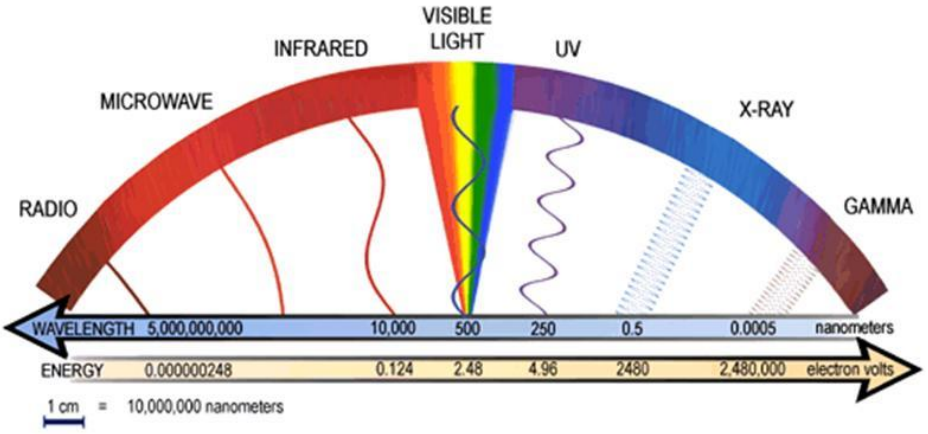

Figure 1.13 The electromagnetic spectrum

1.3.2.1 Neutral State Red Colored Polymers

Neutral state red colored polymers show λ_{max} at ca. 500 nm which corresponds to the absorption at the blue-cyan colored region in the visible spectrum. Although, there are numerous conjugated polymers containing red color in their neutral states, "possessing transmissive state in their oxidized states" that is a significant feature in electrochromic smart windows applications are still unexplored.

The archetype for the neutral state red and oxidized state transmissive materials was from the pyrrole family [34]. A few years ago, poly(3,4-ethylenedioxypyrrole) (PEDOP) was the only material switching between red and transmissive (Figure 1.14). This polymer also represents a unique property such as low lying LUMO level allowing it to be n dopable. Despite these promising features of PEDOP, it lacks solution processability. On account of eliminating that problem via keeping these unique properties, poly(3,4- propylenedioxypyrrole) (PProDOP) was synthesized.

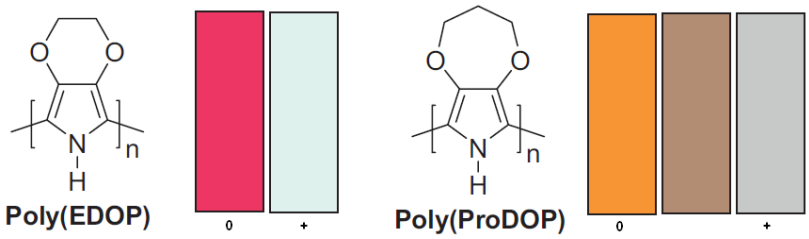

Figure 1.14 Colors and structures of PEDOP and PProDOP

The prominence of structural modification, even minimal, in conjugated polymers can be seen easily with the color changes such as the case for PEDOP and PProDOP. By the addition of one more ethylene unit to the structure of PEDOP, the neutral state color absorption is more blue shifted generating orange color, while the oxidized state becomes highly transmissive. In addition to these superior properties, PProDOP had a mid absorbing state as brown color. The polymer is solution processable though not in sufficient amounts. For this reason, in 2009, Toppare *et al.* reported a solution processable polymer (PTBT), seen in Figure 1.15, switching between red to transmissive by the addition of alkyl substituted benzotriazole (BTz) unit to PTh chain [20].

Herewith, this thiophene coupled Btz containing polymer showed unforeseen characteristics such as switching between all primary colors including black while possessing red as the neutral color and transmissive state when oxidized. Additionally, the polymer is solution processable, fluorescent and both p and n dopable which allows the polymer to be used in a wide range of applications. In brief, with this outstanding breakthrough, a polymer having all desired properties was achieved in a single structure. After this significant contribution to the conjugated polymers, many polymers having BTz on the polymer backbone were developed.

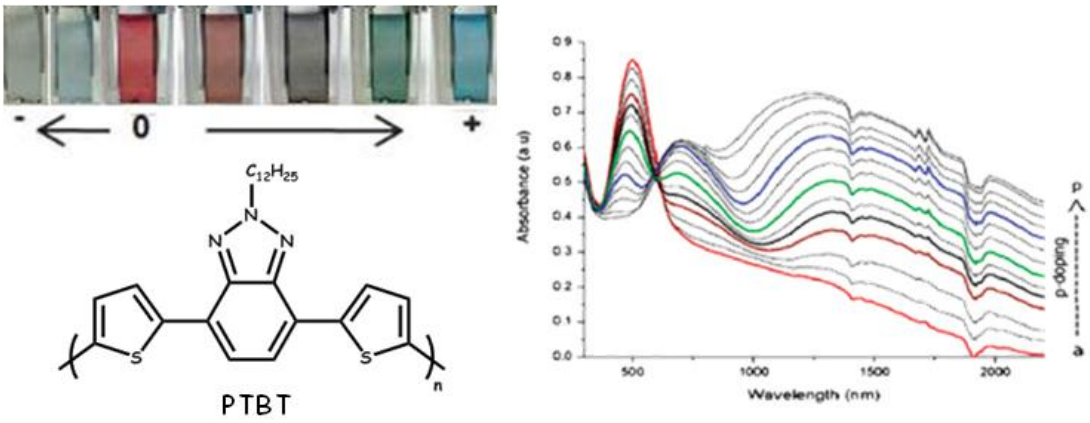

Figure 1.15 Absorption spectra and colors upon oxidation and reduction of PTBT

Recently, solution processable red to highly transmissive colored polymers are introduced. The newest example from Reynolds *et al.* is poly (3,4-di(2-ethylhexyloxy)thiophene-co-3,4-di(methoxy)thiophene) (ECP-red) [35]. ECP-red has steric relaxations due to the coupling of the dialkoxy substituted thiophene with dimethoxy substituted thiophene, while the polymer of 3,4- di(3-ethylhexyloxy)thiophene (ECP-orange) shows orange color in its neutral state. The random incorporation in ECD-red copolymer provides increase in conjugation length by allowing steric interactions causing red shifted neutral state absorbance (Figure 1.16).

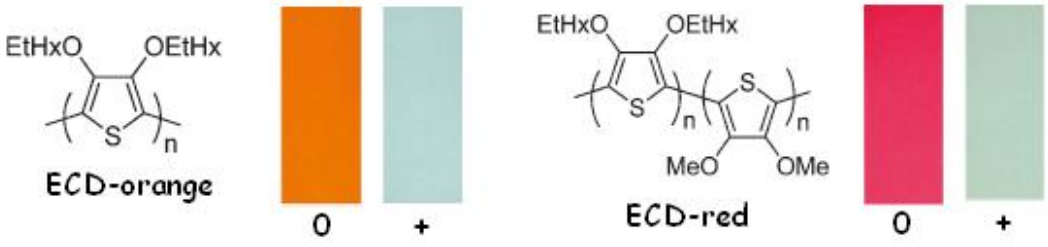

Figure 1.16 Colors and structures of ECD-orange and ECD-red

1.3.2.2 Neutral State Green Colored Polymers

Neutral state green colored materials reveal two distinct λ_{max} at around 400 nm and 700 nm that corresponds to the absorption at both the blue-violet and the yellow-red regions in the visible spectrum. These two distinct absorptions are associated with the π-π* transitions that are attributed to the transitions from the valence band to the antibonding orbital, and to the narrow conduction band [36]. The necessity for the commercialization of the materials pushed researchers to obtain neutral state green colored polymer electrochromics. The challenge in achieving neutral state green colored polymer was covered in 2004 by the phenomenal work of Wudl and Sonmez *et al* (Figure 1.17) [37].

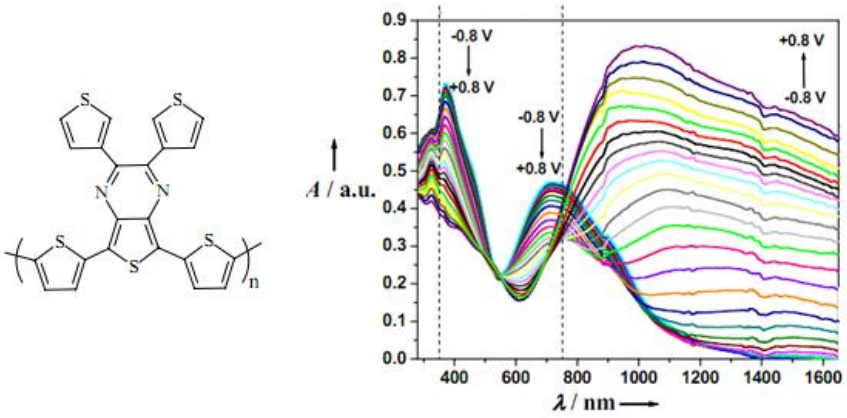

Figure 1.17 The structure and absorption spectrum of PDDTP

The polymer, poly (2,3-di(thien- 3-yl)-5,7-di(thien-2-yl)thieno[3,4-b]pyrazine) (PDDTP), having high green color saturation, an extreme stability and fast switching claimed as a perfect promising material for the electrochromic applications. Despite the fact that the fulfillment of the third leg of color space by electrochemically synthesizing the first neutral green polymer, it was not sufficient to alter the color from green to transmissive in a potential stimulated environment. The oxidized transmissive state is significant in the cause of the attainment the one of three primary colors by keeping others transmissive for

electrochromic device applications. The highly transmissive oxidized sky blue color was accomplished by the superior work of our group in 2007 [38].

The polymer, poly(4,7-di(2,3-dihydro-thieno[3,4-b][1,4]dioxin-5-yl)benzo[1,2,5] thiadiazole) (PBDT), shows two well separated absorption bands at 428 nm and 755 nm with high optical contrast and fast switching time. Despite these promising features of PBDT with green to transmissive sky blue color, it lacks solution processability. Subsequently, the studies over the neutral state green colored polymers were intensified with the syntheses of conjugated polymers by Toppare *et al.* [39] The neutral state green materials still arouse curiosity for the applications in a variety (Figure 1.18).

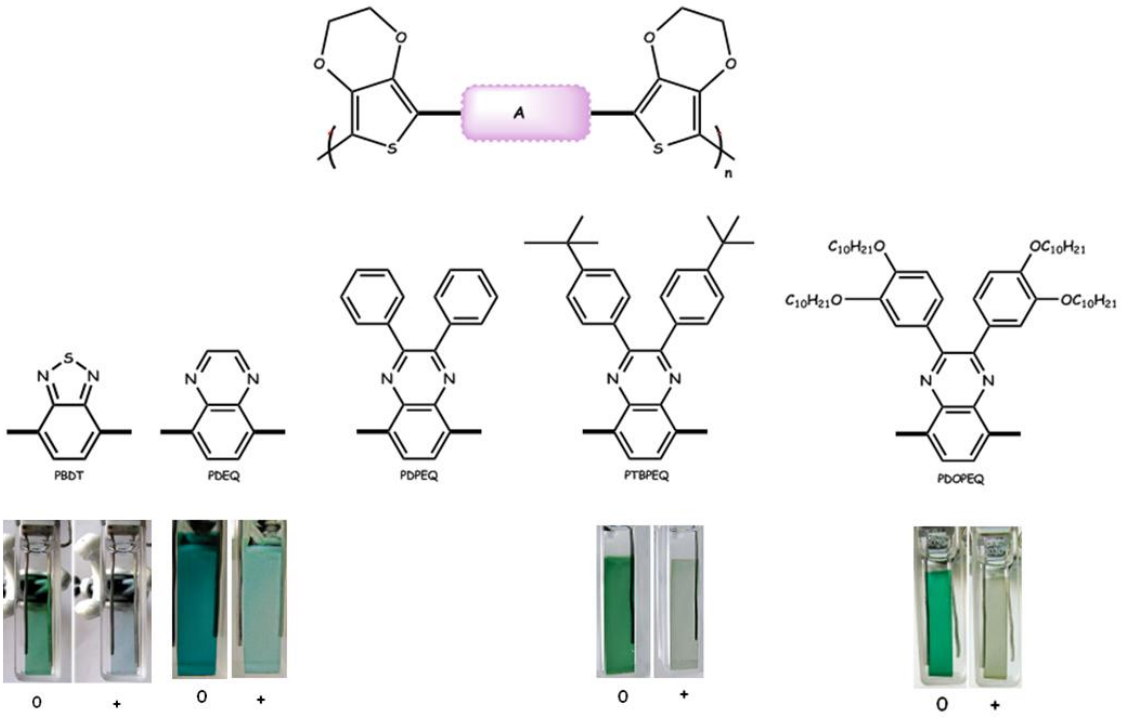

Figure 1.18 The structures and colors of preliminary examples of the neutral state green conjugated polymers

1.3.2.3 Neutral State Blue Colored Polymers

Neutral state absorbances localized to wavelengths longer than 600 nm in the visible spectrum offer blue color. The most prominent example for the neutral state blue and oxidized state transmissive materials was from the thiophene family [40]. Throughout the years, poly(3,4- ethylenedioxythiophene) (PEDOT) , also a well known electron donor unit, was the only material for blue to almost transmissive color switching seen in Figure 1.19. The properties of polymer was not limited to its redox colors, it also represents unique properties such as stability and low band gap allowing better transparency.

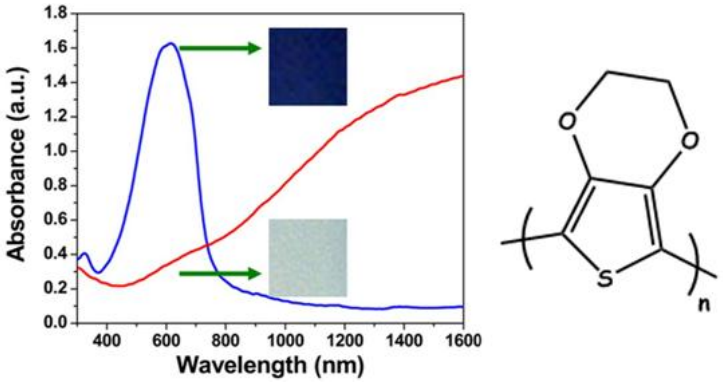

Figure 1.19 The absorbance spectrum for the neutral and oxidized states of PEDOT

Despite these promising features of PEDOT, the lack of processability limits the attraction of the material. In order to eliminate this problem which is a drawback for applications, benzotriazole (Btz) coupled EDOT namely poly(4,7-bis(2,3-dihydrothieno[3,4-b][1,4]dioxin-5-yl)-2-dodecyl-2H-benzo [1,2,3] triazole) (PBEBT) was synthesized acquiring superior properties over parent polymer, PEDOT by Toppare *et al*. [19] In addition to the enhanced electrochromic properties when compared to PEDOT, PBEBT possesses new properties such as high stability and ambipolar characteristics, both p and n dopability with transmissive sky blue switching from neutral state blue color, owing to the electron deficient nature of Btz unit. The drawback remained from PEDOT was

also eliminated with PBEBT; by the solubilizing it with the help of alkyl chains linked to the 2- position of BTz unit [41]. On the account of obtaining electrochemically synthesized, processable and neutral state blue colored polymer, Btz coupled this time with pyrrole donor unit and the results showed that PPyBT achieves this goal [21].

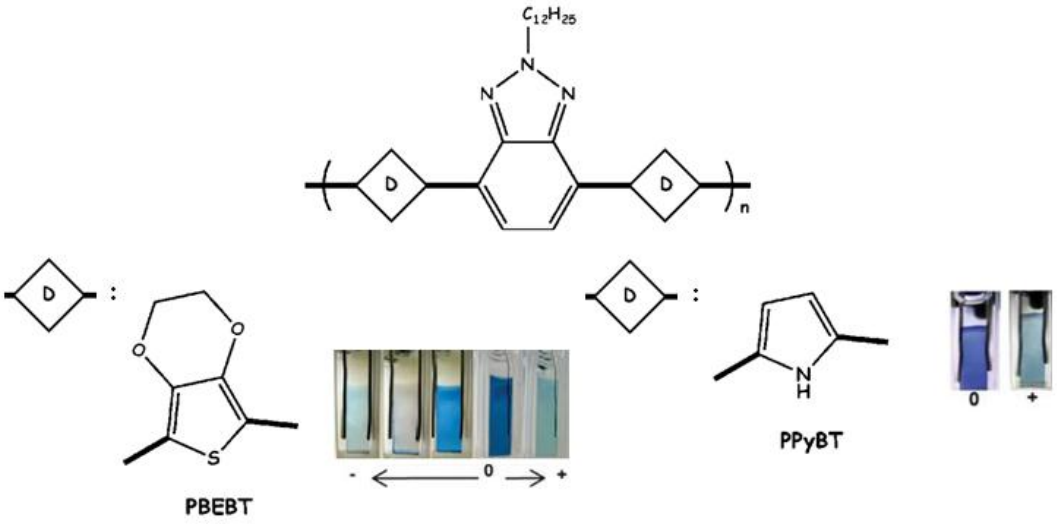

Figure 1.20 The switching colors and structures of PBEBT and PPyBT

In order to have highly transmissive states upon oxidation, Önal *et al.* generated a polymer containing 3,3-didecyl-3,4-dihydro-2H-thieno[3,4-b]-[1,4]dioxepine as the electron rich unit and BTz as the electron deficient unit in the polymer backbone [22]. The polymer has some distinctive properties such as switching between deep blue color and highly transmissive state as well as satisfying solubility due to the additional alkyl chains on the donor unit.

It is worth noting that BTz with a dioxythiophene derivative (DOTs) enables the enhancement in electrochromic properties compare to its benzothiadiazole (BTd) containing DA type counterpart, whose structure represented in Figure 1.21b, reported by Reynolds *et al*. [42] This polymer is also a significant example with its saturated blue color in its neutral state and highly transmissive state in its oxidized state.

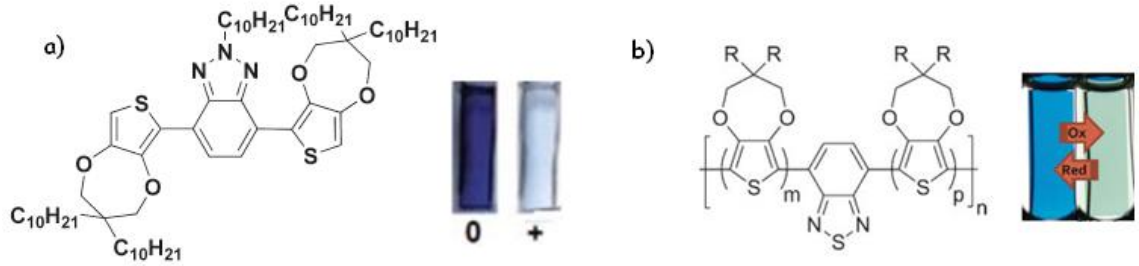

Figure 1.21 The switching colors and structures of a) Btz and b) Btd containing DOT derived conjugated polymers

1.3.2.4 Neutral State Black Colored Polymers

In terms of electrochromic devices, the use of DA type CPs as active layers became more popular over the time due to variety of achievable colors via structural alternations. Electrochromic and non emissive applications of CPs provide a "stimuli effect-free display" in large and flexible devices and they constitute the most important candidates of active materials for future display technologies. During the investigation of soluble, fast switching, high optical contrast and stable CPs for electrochromic devices, neutral state blue, red and green polymers were successfully achieved. Furthermore, introducing the benzotriazole (BTz) bearing CPs into the electrochromic field, solution processable, multi-colored to transmissive switching materials became available for low cost flexible display devices. Having all primary additive colors in different redox states together with a transmissive state made these polymers unique and enormous candidates for ECDs. However, for a possible application of electrochromic polymers, smart windows, black colored conjugated polymers integrated with a transmissive state should have been designed [43]. Besides, in the field of polymeric solar cells these materials which absorb in a broad region of the ultraviolet–visible (UV-vis) spectrum would yield high efficiency since light harvesting is one of the most important parameter for these devices [44].

Spanning the entire visible spectrum, ie, absorbance in a broad range enables the production of neutral state black colored materials. Yet, synthesizing a material covering evenly across the entire visible spectrum in its neutral state

and absorbing only in the infrared, excluding visible region in its oxidized state was a crucial issue. In 2008, Reynolds *et al*. demonstrated that an electrochromic material which is the archetype of switching black to transmissive color by chemical co-polymerization via controlling the repeating unit structures (Figure 1.22) [45]. This copolymer possesses a "low band gap" arising from benzothiadiazoles (BTz) as the electron deficient unit and substituted propylenedioxythiophene (subProDOT) as the electron generous unit switching between a strong opaque black color as neutral form and highly transmissive oxidized form.

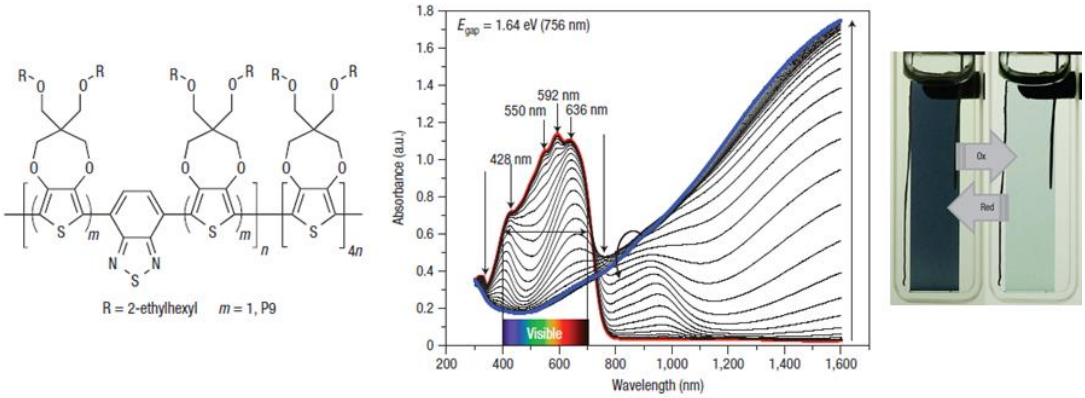

Figure 1.22 The spectroelectrochemistry of the first black neutral state copolymer

Although this copolymer has magnificent features, it complicates the large scale production in consequence of complexity of the synthetic pathway that includes copolymerization with an increased rate of donor and acceptor substituents.

Subsequently, Reynolds *et al.* designed a polymer containing a random mixture of the previous donor-acceptor heterocycles (4,7-dibromo-2,1,3 benzothiadiazole (BTd) with 5-dibromo-3,4-propylenedioxythiophene and 2,5-tributylstannyl-2-ethylhexyloxy- substituted 3,4- propylenedioxythiophene in different feed ratios, via cross coupling polymerization in order to facilitate the synthetic pathway [46].

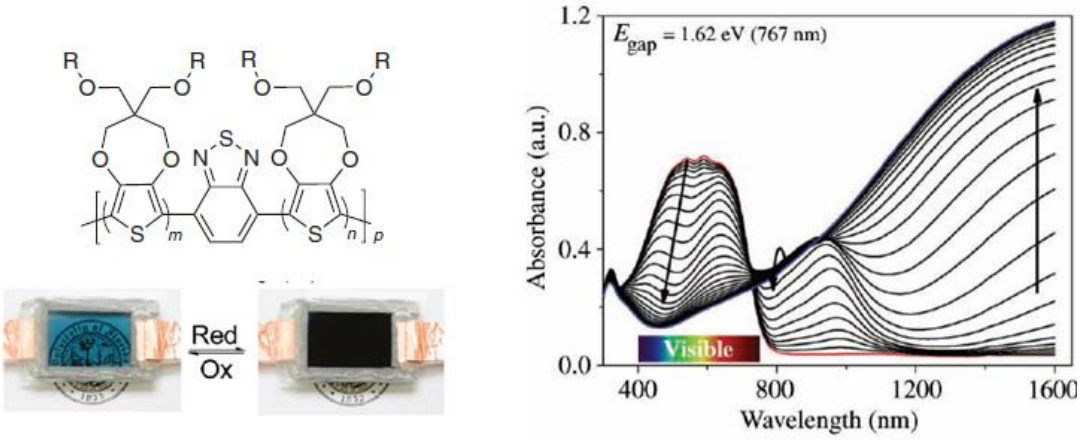

Figure 1.23 The spectral and device properties of easy producible black copolymer

Indeed, to date, there are a few examples for chemically polymerized black neutral state polymers. In addition to these polymers, electrochemically copolymerized black colored polymers can be achieved. Later on Toppare *et al*. discovered a polymer (PTBT) (Figure 1.15) both chemically and electrochemically having black color in addition to all RGB colors; Önal *et al.* reported an electrochemically copolymerized soluble, low band gap black polymer comprising two different monomers designed with respect to the donor acceptor theory, in 2010 [47].

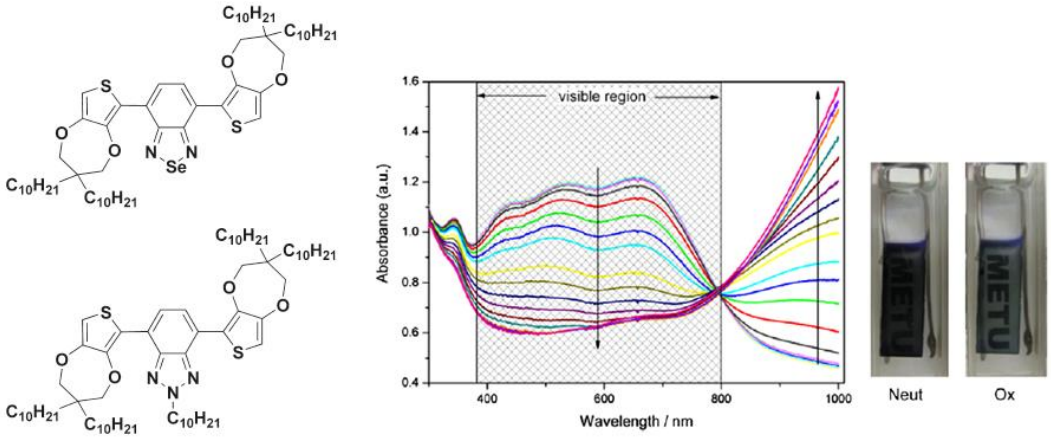

Figure 1.24 The spectroelectrochemistry of the electrochemically synthesized black neutral state copolymer by Önal *et al.*

1.4 Synthesis of Conducting Polymers

Several types of polymerization methods are utilized for the synthesis of conducting polymers [48]. Polymerizations via chemical and electrochemical methods are the most used ones for conducting polymers. The foremost feature of electrochemical polymerization over chemical is the time spent for the synthesis of the polymer. In electrochemical polymerization, polymer is formed in a short time and positively doped when it is formed. Whereas in chemical polymerization the formation of polymer is time consuming and the resulting polymer is in its neutral state.

1.4.1 Chemical Polymerization

Monomer oxidation through the use of transition metal halides and metal catalyzed cross coupling reactions are basically the main methods for the chemical polymerization. Figure 1.25 aims to show these polymerization methods used for the polymerization of thiophene unit, the donor unit of this study [7]. A wide variety of chemical routes using metal catalyzed coupling strategies are performed for the most of the commercially available polymer synthesis based on thiophene.

Sugimoto method, the $FeCl_3$ mediated oxidative polymerization in chloroform as the solvent is known as an efficient way for obtaining high molecular weight polymers with sufficient purity. Sugimoto route is the beneficial strategy for the polymerization of the unsubstituted, as well as 3- alkyl substituted thiophene units, using $FeCl_3$ as the oxidizing agent [49]. Several approaches have been developed to synthesize polythiophenes via metal catalyzed polycondensation reactions. In 1980, the very first and poorly soluble examples for the chemical preparation of polythiophenes (PThs) were reported by two research groups utilizing an extension of Kumada- Corriu coupling. This extension basically was based on the reaction between aryl halides and Grignard reagents (Mg in THF) followed by the subsequent self coupling of the difunctional reagent with itself.

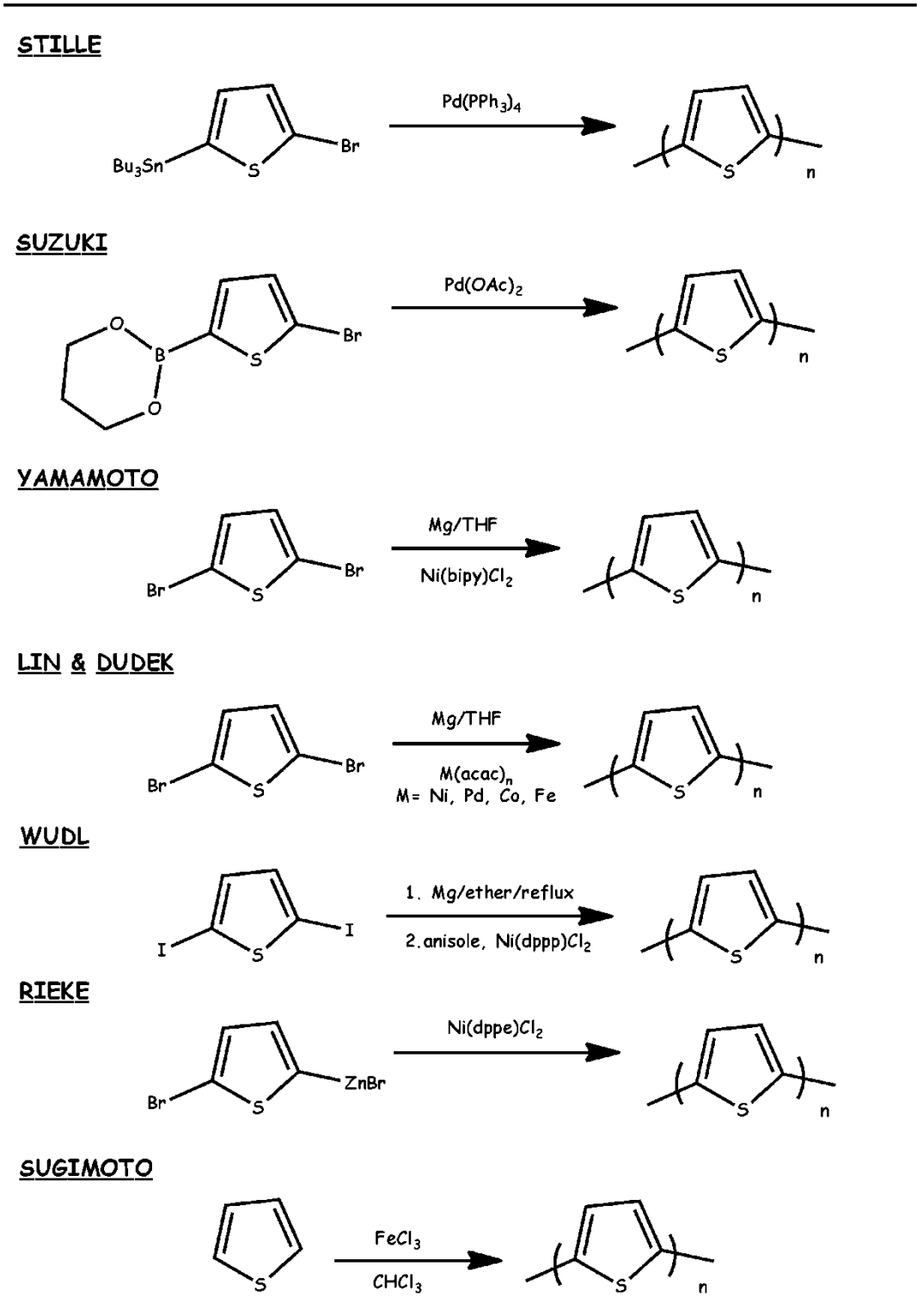

Figure 1.25 Polythiophenes with several polymerization methods

Yamamoto's research group obtained PThs via the reaction between mono-Grignard reagent substituted difunctional thiophene unit (2-bromo-5-magnesio bromothiophene) in the presence of nickel(bipyridine)dichloride ($Ni(bipy)Cl_2$) as catalyst [50]. The second research group, Lin & Dudek's, treated difunctionalized thiophene in the same way with Yamamoto only using several different transition metal acetylacetonate catalysts like $Ni(acac)_2$, $Pd(acac)_2$, $Fe(acac)_2$, $Co(acac)_2$ [51].

Soon after, Wudl *et al*. was reported a synthetic route with the inclusion of Kumada-Corriu type reactions aiming at increasing purity and molecular weight of PThs. This route consists of the formation of difunctionalized thiophene having iodomagnesio group at one end and iodo group at the other from 2,5-diiodothiophene via Grignard reagent. The procedure is then followed by the treatment with hot anisole utilizing nickel(II)(1,3-diphenylphosphinopropane) chloride ($Ni(dppp)Cl_2$) as the catalyst [52]. These extensions on Kumada- Corriu reaction were examined to improve purity of PThs with minimizing metal content. Yamamoto *et al.* reported a polycondensation including 2,5-dihalothiophenes with a catalytic system bearing nickel(II)cyclooctadiene ($Ni(cod)_2$) and triphenylphosphine (PPh_3) in DMF [53].

Due to the insoluble nature of PThs, attempts were centered to make PThs soluble by adding solubilizing pendant alkyl chains so as to improve processability of materials [54]. As a result of these attempts, head to head (HH), head to tail (HT) and tail to tail (TT) couplings were presented.

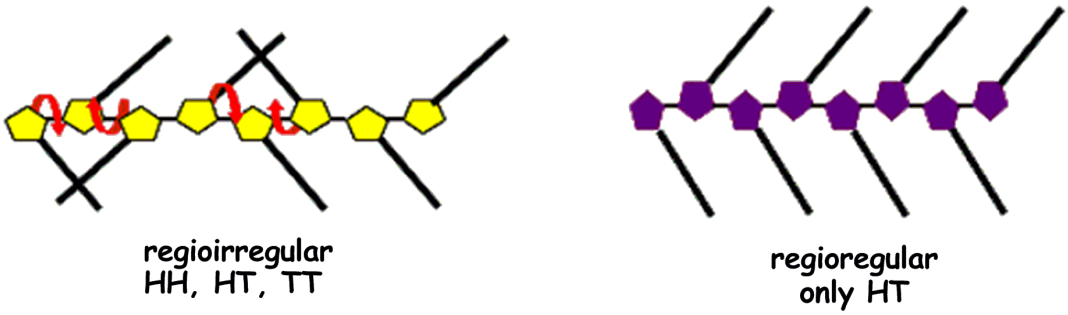

Figure 1.26 Schematic representations of regioirregular and reigoregular polyalkylthiophenes (PAThs)

The interesting work of Rieke *et al.* showed that the choice of the catalyst can alter the product either as regiorandom or regioregular. The Rieke method contains Rieke zinc as the organometallic substituent and in the presence of $Pd(PPh_3)_4$, the structure is mixed HH, HT, TT; regiorandom, while in the presence of $Ni(dppe)Cl_2$, the structure is all HT; regioregular [55].

Palladium catalyzed cross coupling reactions occur with the formation of active species which are carried out in situ by the reduction of palladium source, basically Pd(II) to Pd(0) precursor [56]. The catalysts having palladium as the transition metal differ according to their strong σ donating ligands; $Pd(PPh_3)_2Cl_2$, $Pd(PPh_3)_4$, $Pd_2(dba)_3$, $Pd(OAc)_2$, $Pd(PtBu_3)_2$. σ donating ability of ligands alter the rate of the reaction via facilitating the reversible catalytic cycle so that increasing the electron density around the metal causes rapid oxidative addition of the catalyst to the reagent.

The proposed mechanism of palladium catalyzed cross coupling reactions consists of three steps; oxidative addition, transmetalation and reductive elimination seen in Figure 1.27. In the first step, oxidative addition of the halide component to the palladium(0) ligand complex to form oxidized Pd center with Pd(II) active species. In the transmetalation step, nucleophile bonded to the organometallic substituent is transferred from the metal to the palladium (II) ligand complex, while halide component is carried to the opposite direction. Finally, the Pd(II) complex containing two ligands and two components undergoes reductive elimination in the cause of yielding the product and the starting catalyst Pd(0) for the following cycle.

As a result of the contributions to the "palladium catalyzed cross coupling reactions in organic synthesis" the 2010 Nobel Prize in Chemistry went to Richard Heck, Ei-ichi Negishi and Akira Suzuki [57].

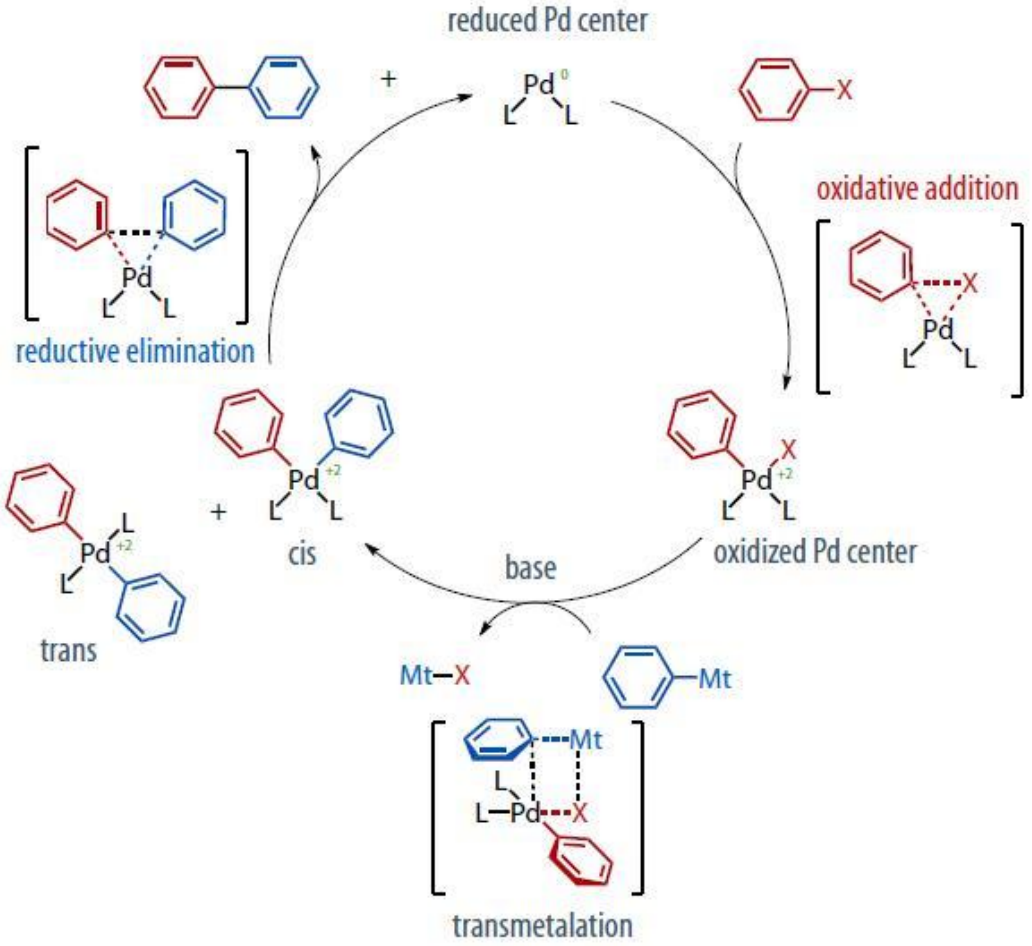

Figure 1.27 Mechanism of palladium catalyzed cross coupling reactions

The palladium mediated coupling reactions take different names with respect to the organometallic reagent component (R-Mt) used. These reagents can be Mg, Cu, Sn, B, Li etc. and cross coupling reactions are entitled with respect to the type of organometallic reagents (Table 1.1). When the organometallic component is Sn metal, the cross coupling reaction gets the name of Stille Coupling. The Stille Coupling uses organostannanes and substituted halides in the presence of palladium catalyst to form product having a versatile carbon-carbon bond formation. Due to the rapid preparation, durability to air and easy purification of organotin compounds, Stille Coupling become so popular over the years. It has only a few limitations such as low polarity causing poor solubility and the toxicity of tin groups [58].

Table 1.1 Transition metal catalyzed cross coupling reactions

COUPLING	**R-Mt**	**R' –X (Alkyl halide)**
HECK	Alkene	aryl,alkenyl,alkyl
KUMADA-CORRIU	R-MgX or R-Li	aryl, alkenyl
NEGISHI	R-ZnX	aryl, alkenyl, alkynyl, acyl
STILLE	R-Sn(alkyl)$_3$	aryl, alkynyl, acyl
SUZUKI	R-B(OH)$_2$	aryl, alkenyl, alkyl
SONIGASHIRA	Alkyne	aryl,alkyl,

In addition to the formation of catalytic carbon-carbon single bond during polymerization via transition metal mediated cross coupling reactions, synthesis of C=C double bonds and C≡ C triple bonds containing polymers are also possible. Mainly, Knoevenagel polycondensation, Wittig-Horner reaction, McMurry coupling and Sonogashira coupling can be mentioned as the leading reactions for the double and triple bond formation on polymerization.

1.4.2 Electrochemical Polymerization

Apart from chemical polymerization reactions, conjugated polymers can be rapidly characterized via electrochemical polymerization method. Material characterization in terms of optical and electrochemical properties is performed with coating the desired polymer on an electrode surface. Electrochemical polymerization allows the oxidation of monomers to polymers in an environment containing an inert electrode (platinum, gold or indium tin oxide coated glass slide) as working electrode, reference electrode, counter electrode and an electrolytic solution containing the monomer in an inactive organic solvent (acetonitrile, dimethylformamide, dimethylsulfoxide) containing a supporting electrolyte (hexafluorophosphates, tetrafluoroborates, perchlorates). In electrochemical anodic polymerization, polymerization occurs directly on an anode and during synthesis, no purification and problems generated due to catalyst happens.

The electrogenerated radical cations are formed during electrochemical polymerization. After a series of radical coupling reactions and electrochemical reactions which is represented by $E(CE)_n$ mechanism, polymer formation occurs [59]. For the thiophene unit, at this time electrochemical polymerization is shown with a proposed mechanism in Figure 1.28.

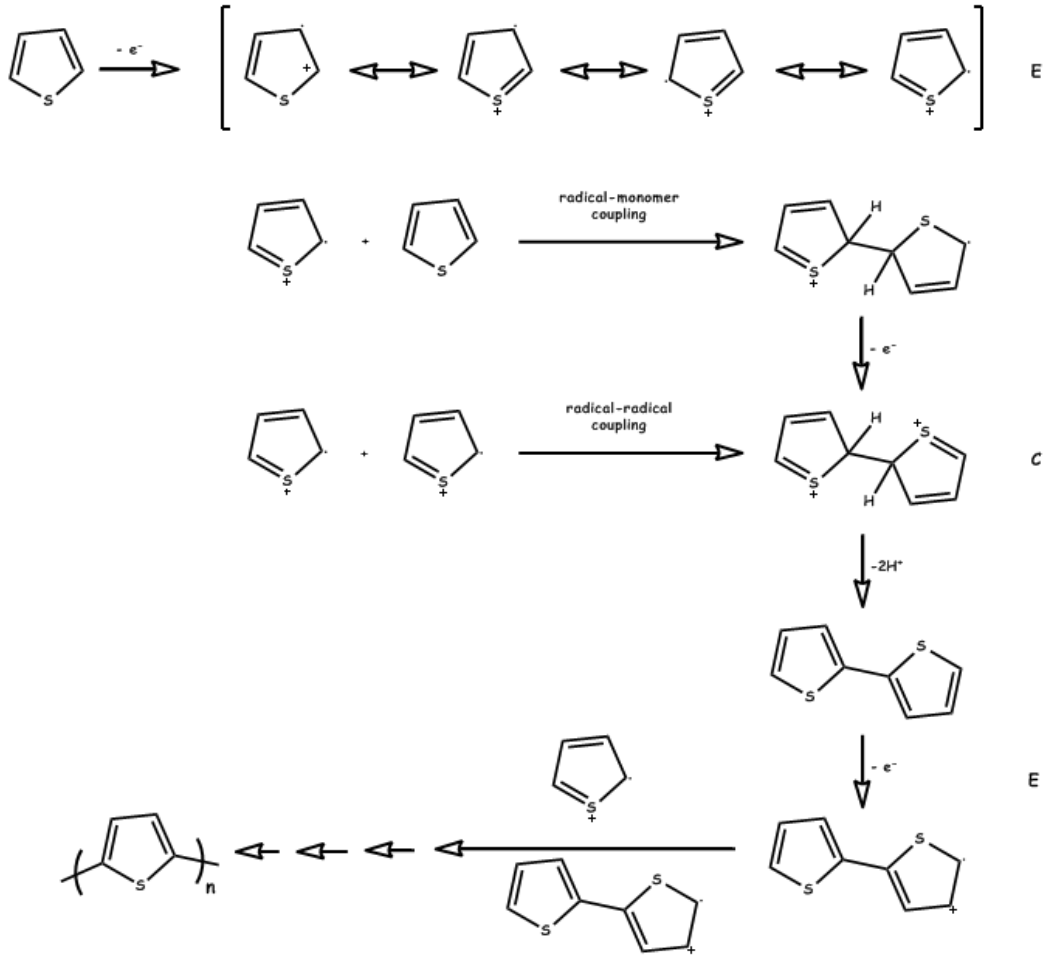

Figure 1.28 Polythiophene via electrochemical polymerization

According to the $E(CE)_n$ mechanism; in the first step that is the electrochemical step, consisting the monomer oxidation via releasing electron and causing the radical cation formation. The resonance stabilized form of the radical cation also occurs. The radical cation concentration is kept continuously higher around the working electrode surface, so that the formation of radical cations is much faster than the monomer diffusion from bulk solution. Owing to this case, the polymerization proceeds easily. The second step, chemical reaction step, consists of the coupling reactions between the radical cations or radical cation and monomer molecule to form a neutral dimer unit with losing rapidly two protons. After the formation of neutral dimer, due to the applied potential, this unit is

oxidized again to form its radical cation and undergoes coupling reaction to form a trimer. With the following reactions occurring both electrochemically and chemically, the long chain structure results in an insoluble oligomer in the electrolytic environment. Thus, this insoluble oligomer covers the working electrode surface and one can say that the desired polymer precipitates onto electrode surface via successive electrochemical and chemical steps.

The resulted polymer film is in its positively doped state, but can have numerous defects as represented for polythiophenes in Figure 1.29 due to the reasons including cross linking, branching and some mislinkages.

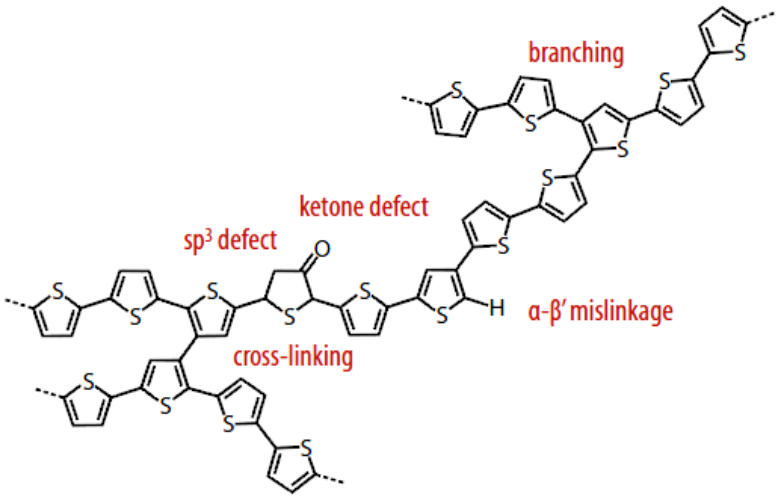

Figure 1.29 The possible defects formed in electrochemical polymerization of PTh

1.5 Alternating and Random Copolymers

Alternating and random copolymers are synthesized in order to satisfy the synthesis of linear structures via organometallic polycondensation methods which proceed selectively through the functional end-groups. In alternating copolymers, polymer chain consists of donor and acceptor segments, respectively.

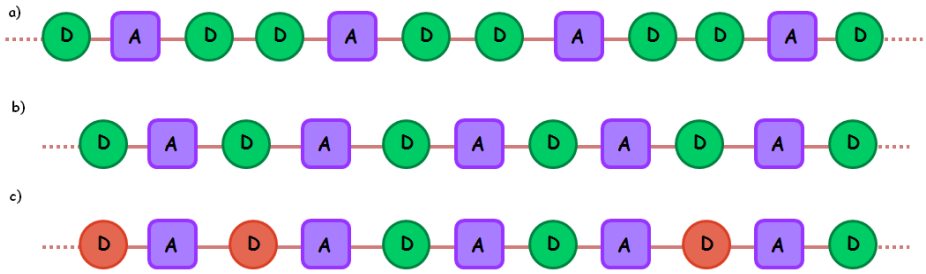

Figure 1.30 Representation of donor-acceptor polymers a) chemically or electrochemically polymerized D-A-D polymers, b) D-A alternating copolymers, c) D-A random copolymers

The only reason to attempt synthesizing alternating copolymer is to provide several properties for the polymers for efficient applications. The benzotriazole-thiophene alternating copolymer, PTBT-DA12, was synthesized via Stille coupling reaction. The alternating polymer shows nearly the same colors with PTBT such as neutral state red color. Taking into account that the alternating copolymer has less donor units than chemically or electrochemically polymerized D-A-D containing ones, in other words alternating copolymer PTBTDA12 has an electron deficient nature compared to PTBT [69]. Due to this reason, the decrease in HOMO energy level, in connection with broadening the energy gap between HOMO and LUMO levels are expected. The increase is seen with the optical band gap values which are 1.65 eV for PTBT and 1.73 eV for the alternating copolymer. Alternating and random copolymers arouse interest nowadays due to their facile synthetic pathways and solution processability.

1.6 Aim of Work

The study is concentrated on the synthesis of donor-acceptor type random copolymers differing by the acceptor units on the polymer backbone in consequence of the achievement of the full visible light absorption. The random copolymers are designed to yield polymer chains possessing alternating DA segments with randomly distributed additional acceptor units that are the variables for all copolymers. The main idea that lies behind having full visible light absorption, visually black color, is the combination of neutral state red and green colored materials. In connection with the difference in absorbed wavelengths between neutral state red and green colored materials, spanning of the entire visible spectrum with the broad and uniform absorption in all visible wavelengths is aimed. For this purpose, 5,8-Dibromo-2,3-bis(4-*tert*-butylphenyl) quinoxaline, 5,8-dibromo-2,3-di(thiophen-2-yl)quinoxaline and 4,7-dibromobenzo [c][1,2,5]selenadiazole units are perceived as additional acceptor units and these constituents are combined with the 4,7-dibromo-2-dodecyl-2H-benzo[d][1,2,3]triazole unit and the 2,5-bis(tributylstannyl)thiophene moiety via Stille coupling.

CHAPTER 2

EXPERIMENTAL

2.1 Materials and Methods

All the components for the synthesis of copolymers were synthesized by following previously published procedures. 5,8-Dibromo-2,3-bis(4-*tert*-butylphenyl)quinoxaline[60], 5,8-dibromo-2,3-di(thiophen-2-yl)quinoxaline[61] and 4,7-dibromobenzo[c][1,2,5] selenadiazole[62] units were separately combined with the 4,7-dibromo-2-dodecyl-2H-benzo[d][1,2,3]triazole [19] unit and the 2,5-bis(tributylstannyl)thiophene [63] moiety via Stille coupling. For the synthesis of the donor acceptor type random copolymers; 2,1,3-Benzothiadiazole (Aldrich), bromine (Br_2) (Merck), hydrobromic acid (HBr, 47%) (Merck), sodium borohydride ($NaBH_4$) (Merck), thiophene (Th) (Aldrich), 4-*tert*-butylbenzaldehyde (Aldrich), 2,2'-thenil (Aldrich), *p*-toluenesulfonic acid (PTSA) (Aldrich), methanol (MeOH) (Aldrich), ethanol (EtOH) (Aldrich), hexane (C_6H_{14}) (Aldrich), chloroform ($CHCl_3$) (Aldrich), dichloromethane (DCM) (Aldrich), n-butyllithium (n-BuLi, 2.5M in hexane) (Acros Organics), tributyltin chloride ($Sn(Bu)_3Cl$, 96%) (Aldrich), selenium dioxide (Merck), diethylether (Et_2O) (Merck), benzotriazole (Fluka), potassium *tert*-butoxide (Aldrich), 1-bromododecane (Aldrich), bis(triphenylphosphine)palladium(II) dichloride (Aldrich) were used as received. Tetrahydrofuran (THF) (Fisher) was used after dried with benzophenone (Merck) and sodium prior to use.

2.2 Equipment

^1H NMR spectra referenced to tetramethylsilane were recorded in $CDCl_3$ on Bruker Spectrospin Avance DPX-400 Spectrometer. Electrochemical studies were

performed in a three electrode cell consisting of an Indium Tin Oxide doped glass slide (ITO) as the working electrode, platinum wire as the counter electrode, and Ag wire as the pseudo reference electrode under ambient conditions using a Voltalab 50 potentiostat. The reference electrode and all the results were subsequently calibrated to Fc/Fc^{+} and the band energies were calculated relative to the vacuum level considering that the value of NHE is -4.75 eV vs. vacuum [64]. Spectroelectrochemical studies for copolymers were carried out by using Varian Cary 5000 UV–Vis spectrophotometer. Average molecular weights of copolymers were determined in tetrahydrofuran (THF) via gel permeation chromatography (GPC) on a Polymer Laboratories PL-GPC 220 by using PS standard calibration method.

2.3 Procedure

2.3.1 Synthesis random copolymers

All reagents were obtained from commercial sources and were used without further purification unless otherwise mentioned. The synthetic route to each of alternating copolymers CoP1, CoP2 and CoP3 consists of three components; two of them are main constituents, 4,7-dibromo-2-dodecyl-2H-benzo[d][1,2,3] triazole and the 2,5-bis(tributylstannyl)thiophene moieties, and the rest is the changing additional acceptor units for each copolymers.

2.3.1.1 Synthesis of 4,7-dibromobenzothiadiazole (1)

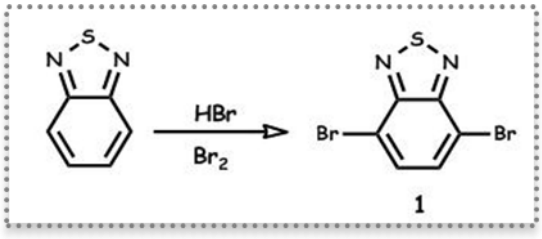

Figure 2.1 Bromination of benzothiadiazole (1).

Benzothiadiazole (2.0 g, 0.015mol) was dissolved in HBr (36 mL) in a reaction flask. Then, a solution of Br_2 (2.0 mL) in HBr (16 mL) was added drop-wise to the mixture. With the first addition, reaction mixture generated orange crystals. After the addition was completed, the mixture was refluxed for 12 h. At the end of the period of time, the reaction mixture was cooled to room temperature. The precipitate was filtered and with the addition of $NaHCO_3$ in water, the excess bromine was removed. The material was dissolved in dichloromethane and extracted with water. The organic residue dried over $MgSO_4$ and the obtained crude product was obtained as a yellow solid in yield 90% (3.9 g, 13.22 mmol). ^{1}H NMR (400 MHz, $CDCl_3$) δ 7.66 (s, 2H). ^{13}C NMR (101 MHz, $CDCl_3$) δ 152.9, 132.3, 113.9.

2.3.1.2 Synthesis of 3,6-dibromobenzene-1,2-diamine (2)

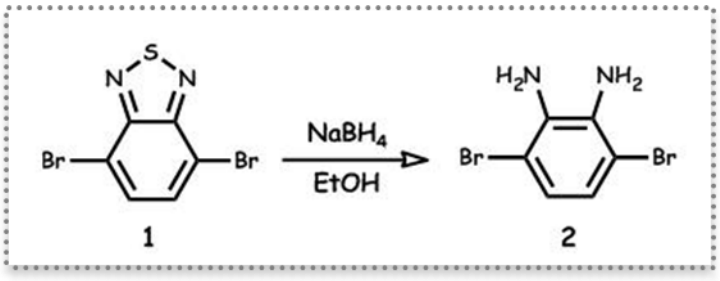

Figure 2.2 Reduction of 4,7-dibromobenzothiadiazole (2).

4,7-Dibromobenzothiadiazole (**1**) (2.5 g, 8.50 mmol) and EtOH (80 ml) were added to a reaction flask. After dissolution, $NaBH_4$ (6.0 g, 0.16 mol) was added slowly to the mixture for 4 h at 0 ^{o}C. When the addition was completed, the mixture was left at room temperature for 12 h. Subsequently, the reaction solvent was removed and crude product was extracted in the presence of diethylether and brine solution. The organic layer was dried over $MgSO_4$ and the residual solvent was removed under vacuum and the crude product was obtained as a pale gray solid (**2**) in yield 80% (1.8 g, 6.72 mmol). ^{1}H NMR (400 MHz, $CDCl_3$) δ 6.78 (s, 2H), 3.82 (s, 4H). ^{13}C NMR (101 MHz, $CDCl_3$) δ 133.5, 123.2, 109.5.

2.3.1.3 Syntheses of additional acceptor units (3-5)

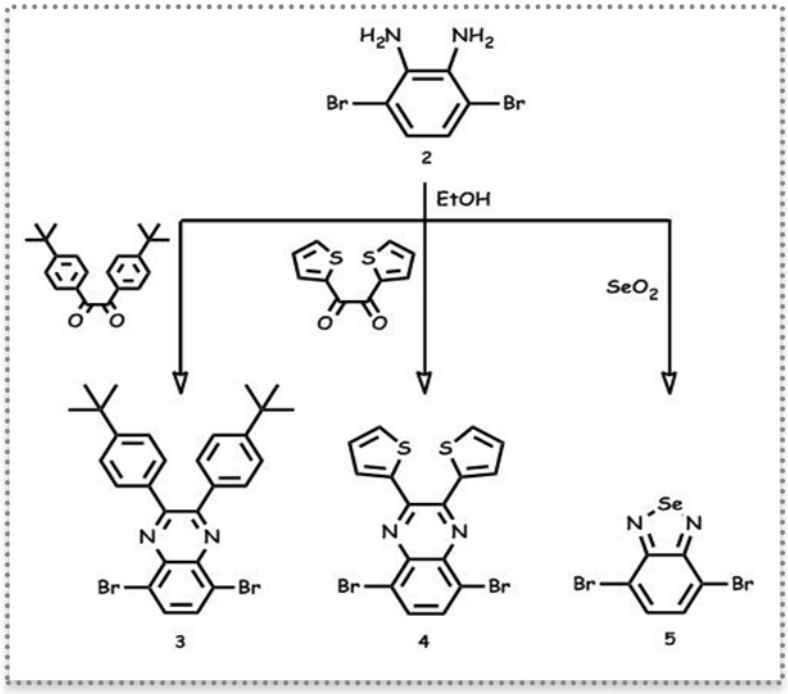

Figure 2.3 Synthetic route for the additional acceptor units (3-5).

2.3.1.3.1 Synthesis of 5,8-dibromo-2,3-bis(4-tert-butylphenyl) quinoxaline (3)

3,6-Dibromobenzene-1,2-diamine (200 mg, 0.752 mmol) and 1,2-bis(4-*tert*-butylphenyl)ethane-1,2-dione (490 mg, 1.88 mmol) were dissolved in ethanol (25 ml) as the reaction solvent. The mixture was heated for few minutes, and then a catalytic amount of PTSA was added. The desired compound was precipitated just after the addition of PTSA. The mixture was refluxed overnight at 100 ^{o}C. The formed precipitate was filtered to obtain white solid. ^{1}H (400 MHz, $CDCl_3$, δ): 7.81 (s, 2H), 7.55 (d, 4H), 7.32 (d, 4H), 1.27(s, 18H).

2.3.1.3.2 Synthesis of 5,8-dibromo-2,3-di(thiophen-2-yl) quinoxaline (4)

3,6-Dibromobenzene-1,2-diamine (200 mg, 0.752 mmol) and 2,2'- thenil (334 mg, 1.88 mmol) were dissolved in ethanol(25 ml) as the reaction solvent. The mixture was heated for few minutes, and then catalytic amount of PTSA was added. The desired compound was precipitated just after the addition of PTSA. The mixture was refluxed overnight at 100 ^{o}C. The precipitate was filtered to obtain yellow solid. ^{1}H (400 MHz, $CDCl_3$, δ): 7.77 (s, 2H), 7.49 (dd, 2H), 7.41 (dd, 2H), 6.98 (s, 2H).

2.3.1.3.3 Synthesis of 4,7-dibromobenzo[c][1,2,5] selenadiazole (5)

3,6-Dibromobenzene-1,2-diamine (200 mg, 0.752 mmol) and SeO_2 (165 mg, 1.88 mmol) were dissolved in ethanol(25 ml) as the reaction solvent. The mixture was heated for few minutes, and then catalytic amount of PTSA was added. The desired compound was precipitated just after the addition of PTSA. The mixture was refluxed overnight at 100 ^{o}C. The formed precipitate was filtered to obtain yellow solid. ^{1}H (400 MHz, $CDCl_3$, δ): 7.58 (s, 2H).

2.3.1.4 Synthesis of 2-dodecyl-2H-benzo[d][1,2,3]triazole (6)

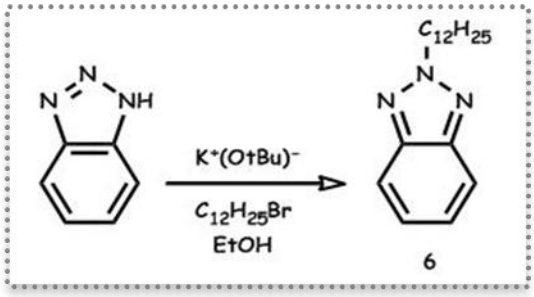

Figure 2.4 Alkylation of benzotriazole (6).

Benzotriazole (5.0 g, 42 mmol), 1-bromododecane (12.2 g, 49 mmol) and potassium *tert*-butoxide (5.0 g, 44 mmol) were refluxed for 12 h in the presence of methanol (50 ml). After the evaporation of solvent, the material was dissolved in chloroform and extracted with water. The organic residue dried over $MgSO_4$ and the obtained crude product was purified by column chromatography over silica gel 3:2 (chloroform: hexane) to obtain **6** as colorless oil in yield 30%. The product became solid when hold in fridge for nearly 12 h. ^1H (400 MHz, $CDCl_3$, δ): 7.86 (d, 2H), 7.35 (d, 2H), 4.71 (m, 1H), 2.10 (m, 2H), 1.3-1.2 (m, 18H), 0.87 (m, 3H).

2.3.1.5 Synthesis of 4,7-dibromo-2-dodecyl-2H-benzo[d][1,2,3]triazole (7)

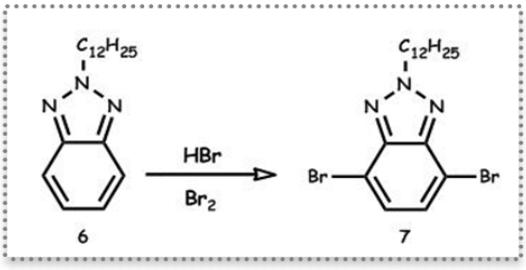

Figure 2.5 Bromination of 2-dodecyl-2H-benzo[d][1,2,3]triazole (7).

2-Dodecyl-2H-benzo[d][1,2,3]triazole (3.7 g, 13.1 mmol) was dissolved in 47 % HBr (5.8 M, 15ml) and the mixture was stirred for one hour at 100 ^0C. After stirring, addition of bromine (5.9 g, 36 mmol) was completed and the reaction flask was heated for 12 h at 135 ^0C. The reaction mixture was then cooled to room temperature and with the addition of $NaHCO_3$ in water, excess bromine was removed. The material was dissolved in chloroform and extracted with water. The organic residue dried over $MgSO_4$ and the obtained crude product was purified by column chromatography over silica gel 1:1 (chloroform: hexane) to obtain **7** as light yellow oil in yield 70%. The product became solid when hold in fridge for nearly 12 h. ^1H (400 MHz, $CDCl_3$, δ): 7.37 (s, 2H), 4.70 (m, 2H), 2.06 (m, 2H), 1.18 (m, 18H), 0.81 (m,3H).

2.3.1.6 Synthesis of 2,5-bis(tributylstannyl)thiophene (8)

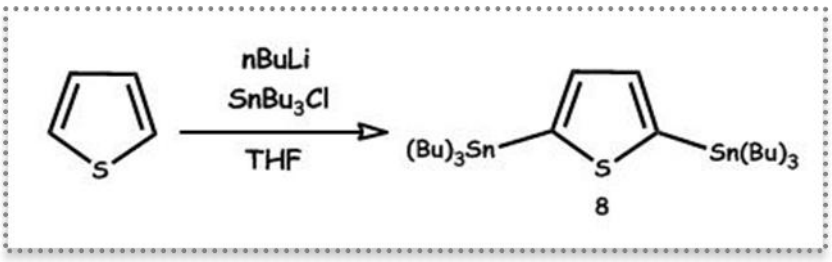

Figure 2.6 Stannylation of thiophene (8).

Thiophene (2.1 g, 25 mmol) was dissolved in dry THF (20 ml) in a round bottom flask under argon atmosphere and vacuumed for 5 min. n-BuLi (22 ml, 2.5 M in hexane) was added dropwise to the solution. After addition was completed, the resulting orange mixture was refluxed for nearly 1 h at room temperature. After 1 hr, the yellow mixture was cooled to room temperature and $Sn(Bu)_3Cl$ (18.0 g, 55 mmol) was added rapidly in one step. After stirring overnight, the solvent was evaporated and the product was extracted with $CHCl_3$ and water. Organic layer was dried over $MgSO_4$ and the solvent was removed under vacuum. The obtained crude product was purified by flash column chromatography over neutral alumina with hexane to obtain **8** as colorless oil in yield 75%. ^1H NMR (400 MHz, $CDCl_3$) δ 7.25 (s, 2H), 1.5 (m, 12H), 1.27 (m, 12H), 1.02 (m, 12H), 0.82 (m, 18H). ^{13}C NMR (100 MHz, $CDCl_3$) δ 140.5, 134.9, 28.06, 26.29, 12.63, 9.91.

2.3.1.7 Synthesis of copolymer 1 (CoP1)

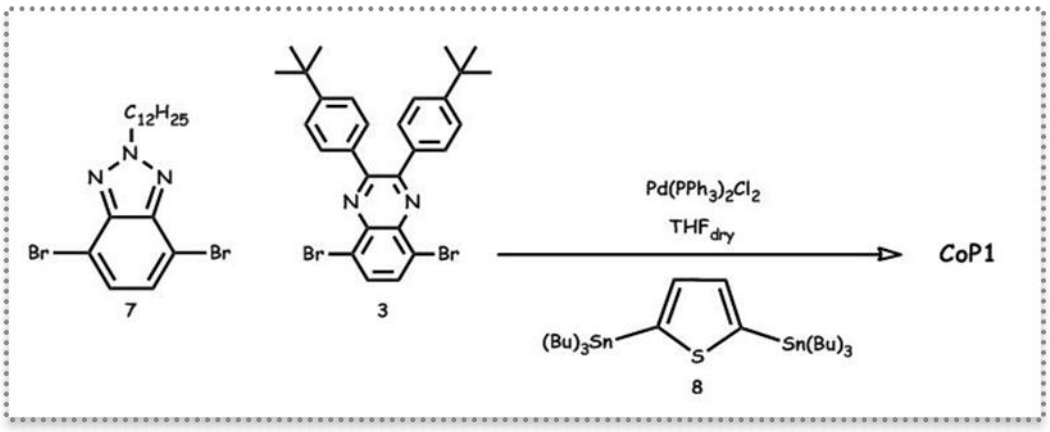

Figure 2.7 Synthetic route for copolymer 1 (CoP1).

Equivalent moles of 5,8-dibromo-2,3-bis(4-*tert*-butylphenyl)quinoxaline (0.186 g, 0.338 mmol) and 4,7-dibromo-2-dodecyl-2H-benzo[d][1,2,3]triazole (0.150 g, 0.338 mmol) and 2,5-bis(tributylstannyl)thiophene (0.450 g, 0.678 mmol) were mixed in dried THF (70 ml) in the presence of $Pd(PPh_3)_2Cl_2$ (70 mg, 0.100 mmol) as the catalyst and refluxed overnight under argon atmosphere. Thereafter, the solvent was removed under vacuum; product was washed with methanol and acetone several times to remove the short chain oligomers and remnant catalyst. CoP1 was obtained as purple solid. GPC (THF): M_w = 29 258 g mol^{-1}, M_n = 18 703 g mol^{-1}, M_z = 42 748 g mol^{-1}, *polydispersity index* = 1.56. ^{1}H NMR (400MHz, $CDCl_3$, δ): 7.9 (benzotriazole), 7.7 (quinoxaline), 7.3 (thiophene), 7.0 (benzene), 4.7 (N-CH_2), 2.2 (C-CH_2), 1.9-0.5 (pendant alkyl chains).

2.3.1.8 Synthesis of copolymer 2 (CoP2)

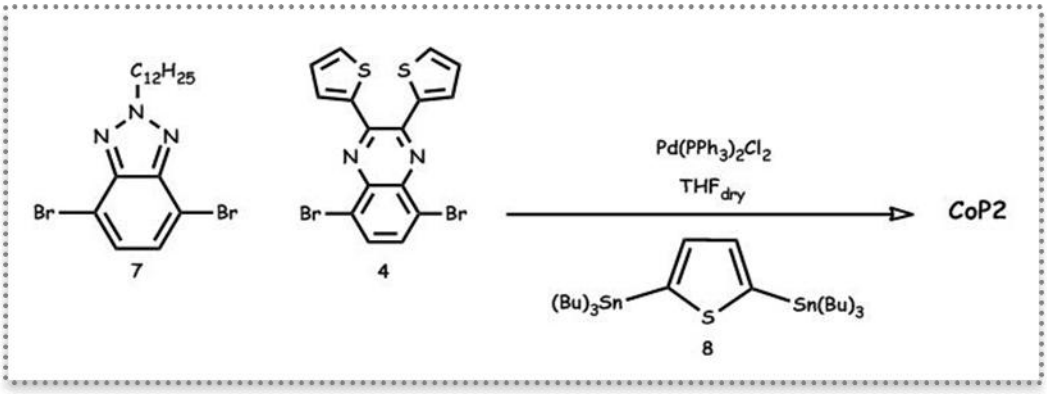

Figure 2.8 Synthetic route for copolymer 2 (CoP2).

In order to synthesize CoP2, same procedure was followed given for CoP1 using 5,8-dibromo-2,3-di(thiophen-2-yl)quinoxaline (0.152 g, 0.338 mmol), 4,7-dibromo-2-dodecyl-2H-benzo[d][1,2,3]triazole (0.150 g, 0.338 mmol) and 2,5-bis(tributylstannyl)thiophene (0.450 g, 0.678 mmol). CoP2 was obtained as a black solid. GPC (THF): M_w = 66 871 g mol^{-1}, M_n = 15 640 g mol^{-1}, M_z = 235 751 g mol^{-1}, *polydispersity index* = 4.28. ^{1}H NMR (400MHz, $CDCl_3$, δ): 7.6 (benzotriazole), 7.5 (quinoxaline), 7.3 (thiophene), 7.0 (thiophene), 6.9 (thiophene), 6.5 (thiophene), 4.6 (N-CH_2), 2.1 (C-CH_2), 1.8-0.8 (pendant alkyl chains).

2.3.1.9 Synthesis of copolymer 3 (CoP3)

The above procedure was followed for the synthesis of CoP3 using 4,7-dibromobenzo[c][1,2,5]selenadiazole (0.115 g, 0.338 mmol), 4,7-dibromo-2-dodecyl-2H-benzo[d][1,2,3]triazole (0.150 g, 0.338 mmol) and 2,5-bis(tributylstannyl)thiophene (0.450 g, 0.678 mmol). CoP3 was obtained as a purplish brown solid. GPC (THF): M_w = 38 317 g mol^{-1}, M_n = 7 896 g mol^{-1}, M_z = 133 133 g mol^{-1}, *polydispersity index* = 4.85. ^{1}H NMR (400MHz, $CDCl_3$, δ): 7.8

(benzotriazole), 7.4 (benzoselenadiazole), 7.0 (thiophene), 5.0 (N-CH_2), 2.0 (C-CH_2), 1.5-0.7 (pendant alkyl chains).

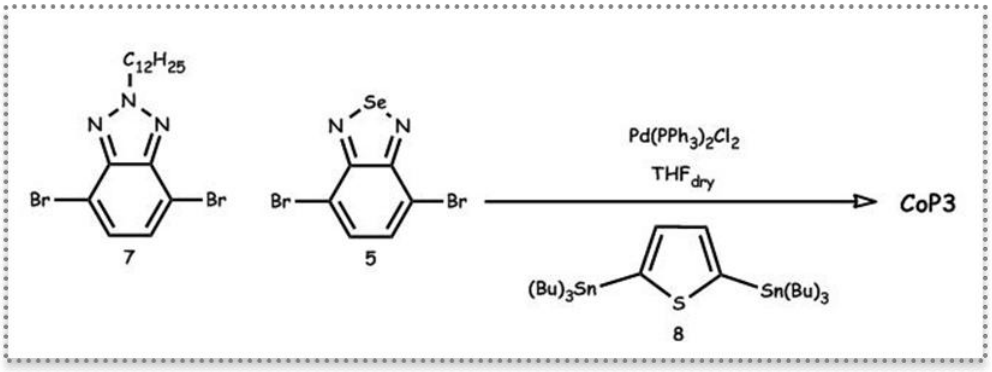

Figure 2.9 Synthetic route for copolymer 3 (CoP3).

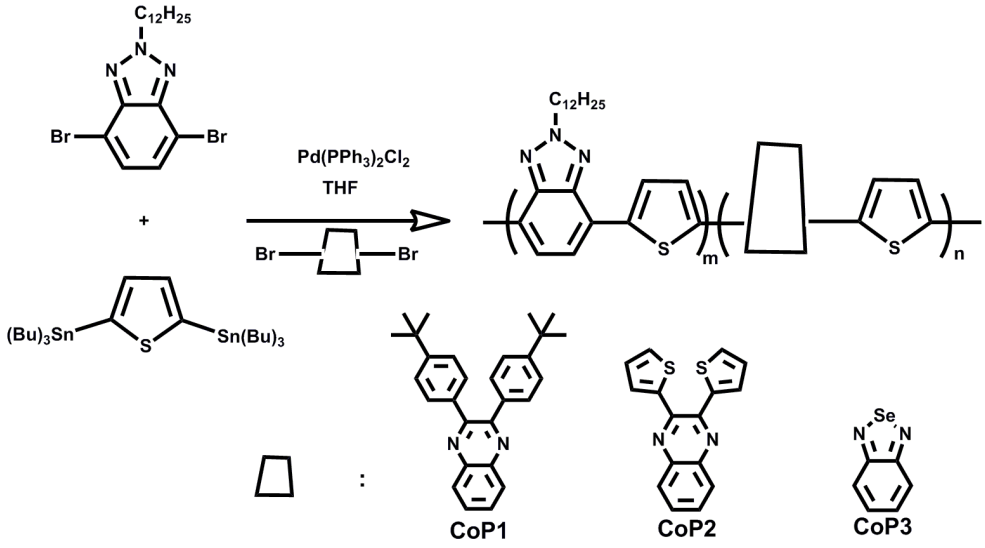

Figure 2.10 General synthetic pathway for all three random copolymers (CoP1, CoP2, CoP3)

CHAPTER 3

RESULTS & DISCUSSION

3.1 Electrochemical Characterization of Random Copolymers

In this study, synthesis and preliminary optoelectronic properties of a series of DA type polymers differing by the acceptor units in the polymer backbone were reported. Polymers CoP1, CoP2 and CoP3 were designed to yield alternating DA segments with randomly distributed different acceptor units along polymer backbone.

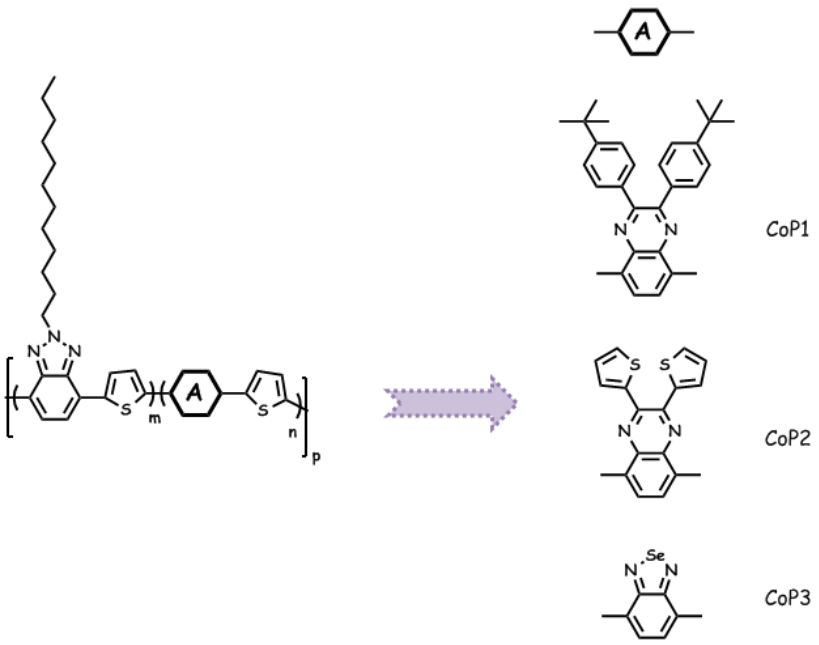

Figure 3.1 Structures of additional electron deficient units for CoP1, CoP2, CoP3

Polymers were obtained via Stille cross coupling reaction between di-stannylated thiophene and di-brominated acceptors. The additional acceptor units; 5,8-dibromo-2,3-bis(4-*tert*-butylphenyl)quinoxaline, 5,8-dibromo-2,3-di(thiophen-2-yl)quinoxaline and 4,7-dibromobenzo[c][1,2,5]selenadiazole were shown in detail in Figure 3.1. Long alkyl chain substituent at 2-N position of benzotriazole (BTz) units served as solubilizing agents for these polymers.

Alternating copolymers of benzoquinoxalines or benzoselenadiazole with thiophene unit without BTz units were not as soluble as required in common organic solvents such as chloroform, THF etc. For that reason, the alternating copolymers of these additional acceptor units (Figure 3.2) could not be characterized electrochemically.

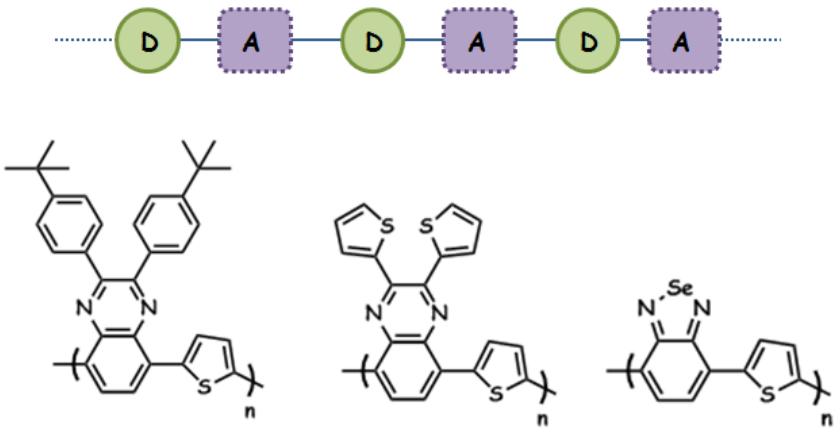

Figure 3.2 Structures of alternating copolymers of additional acceptor units

CoP1, CoP2 and CoP3 were characterized by 1H-NMR (see appendix A) and GPC (see experimental) studies prior to the electrochemical, spectral studies. There was no significant difference in the solubility of these three random copolymers in chloroform and they were spray coated on indium tin oxide (ITO) coated glass slides from 5 mg/ml solutions in chloroform under ambient conditions. On the other hand, the lowest polydispersity index (PDI) for CoP1 suggests different acceptor units, 4,7-dibromo-2-dodecyl-2H-benzo[d][1,2,3]

triazole and 5,8-dibromo-2,3-bis(4-*tert*-butylphenyl) quinoxaline have similar reactivities throughout the polycondensation reaction. In order to determine the electroactivity and oxidation reduction potentials of copolymers, cyclic voltammetry was used. All electrochemical studies were performed in three electrode cells using ITO as the working, Pt wire as the counter and Ag wire (0.3V vs Fc/Fc^{+}) as the pseudo reference electrodes. The potentials were swept between 1.5 V and -2.0 V vs Ag wire. During cyclic potential scan, CoP1 showed the lowest oxidation potential whereas stronger electron acceptor benzoselenadiazole unit in CoP3 increased the oxidation potential of the copolymer (Figure 3.3). Oxidation potentials of polymers are correlated with increasing electron deficiency of the additional acceptor unit on polymer backbone. Besides, GPC studies revealed that longest polymer chains were achieved with CoP1 which also revealed low redox potential.

All polymers were shown to be n-type dopable at negative potentials in 0.1 M $TBAPF_6$/ACN solution under ambient conditions. Strong electron accepting ability of benzoselenadiazole in CoP3 resulted in the lowest n-doping potential among all three as -1.77 V. Ambipolar character of polymers provides estimation of HOMO-LUMO energy levels electronically from the onset potentials of the oxidation and/or reduction potentials for polymers. Inset table in Figure 3.3 summarizes the redox potentials and HOMO-LUMO for polymer films. Electronic band gaps of the polymers were determined as 1.67, 1.76 and 1.82 eV for CoP1, CoP2 and CoP3 respectively from the HOMO-LUMO values determined electrochemically.

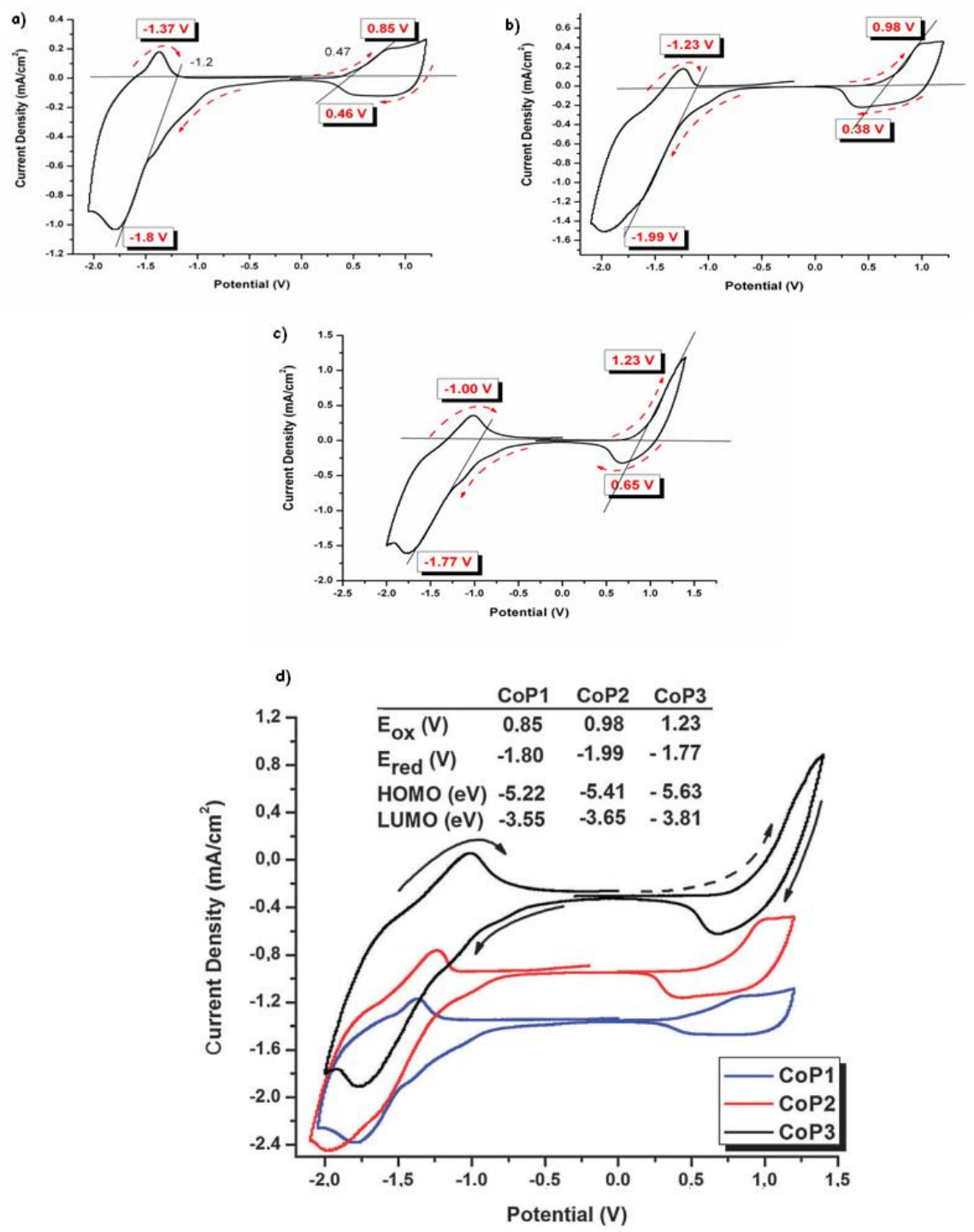

Figure 3.3 CVs and onset potentials of a) CoP1, b) CoP2, c) CoP3 and d) oxidation/reduction potentials and HOMO-LUMO levels of polymer films vs. Fc/Fc^+ in 0.1 M $TBAPF_6$/ACN.

3.2 Spectroelectrochemistry of Random Copolymers

The electrochemical and spectroscopic techniques can be operated at the same time on behalf of determining absorbance changes arising from the electronic transitions of material throughout the oxidation reduction process. The study aims to obtain neutral state black copolymers which can only occur with uniform absorption of the entire visible spectrum. In order to obtain full visible absorption, different oligomers absorbing in different regions of the spectrum were combined. Copolymers were designed to reveal mixed colors of different oligomer segments. To achieve full visible absorption, green (absorption at 400 nm and 700 nm) and red (absorption at 500 nm) materials were combined. Benzoquinoxaline or benzoselenadiazole containing polymers were shown to be green in their neutral states in previous studies. It is well known that neutral state green conjugated polymers reveal two distinct λ_{max} maxima at around 400 and 700 nm. 5,8-Dibromo-2,3-bis(4-*tert*-butylphenyl)quinoxaline coupling with thiophene results in D-A-D electrochemically or chemically polymerized polymer [65]. This polymer shown in Figure 3.4a, possesses two well separated, distinct π-π* transitions arising at roughly 400 nm and 650 nm. These two transitions are claimed as essential to attain neutral state green color. This polymer (PTBPTQ) reveals greenish blue color in its neutral form, upon oxidation the polymer coated ITO electrode takes the color of gray. The D-A-D type electrochemically or chemically polymerizable molecule, PTTQ (Figure 3.4b), was prepared via coupling 5,8-dibromo-2,3-di(thiophen-2-yl)quinoxaline with thiophene [66]. PTTQ represents two distinct π-π* transitions at 400 nm and 654 nm inducing green color at neutral form. Owing to the simultaneous diminishment in the absorptions at 400 nm and 654 nm during oxidation, the oxidized state of the PTTQ becomes transmissive. The optical bandgap calculated from the onset of λ_{max} is 1.28 eV and this polymer shows an outstanding optical contrast of 98 % in NIR region. The last additional acceptor unit containing D-A-D polymer (PTSeT, Figure 3.4c) was synthesized by coupling 4,7-dibromobenzo[c][1,2,5] selenadiazole with thiophene [67]. The PTSeT film was blue-green colored with two well-separated absorption bands at 350 nm and 600 nm. During oxidation, while these absorption bands decreases concurrently, the absorption band at 962 nm advances as polaron formation occurs on the polymer chain.

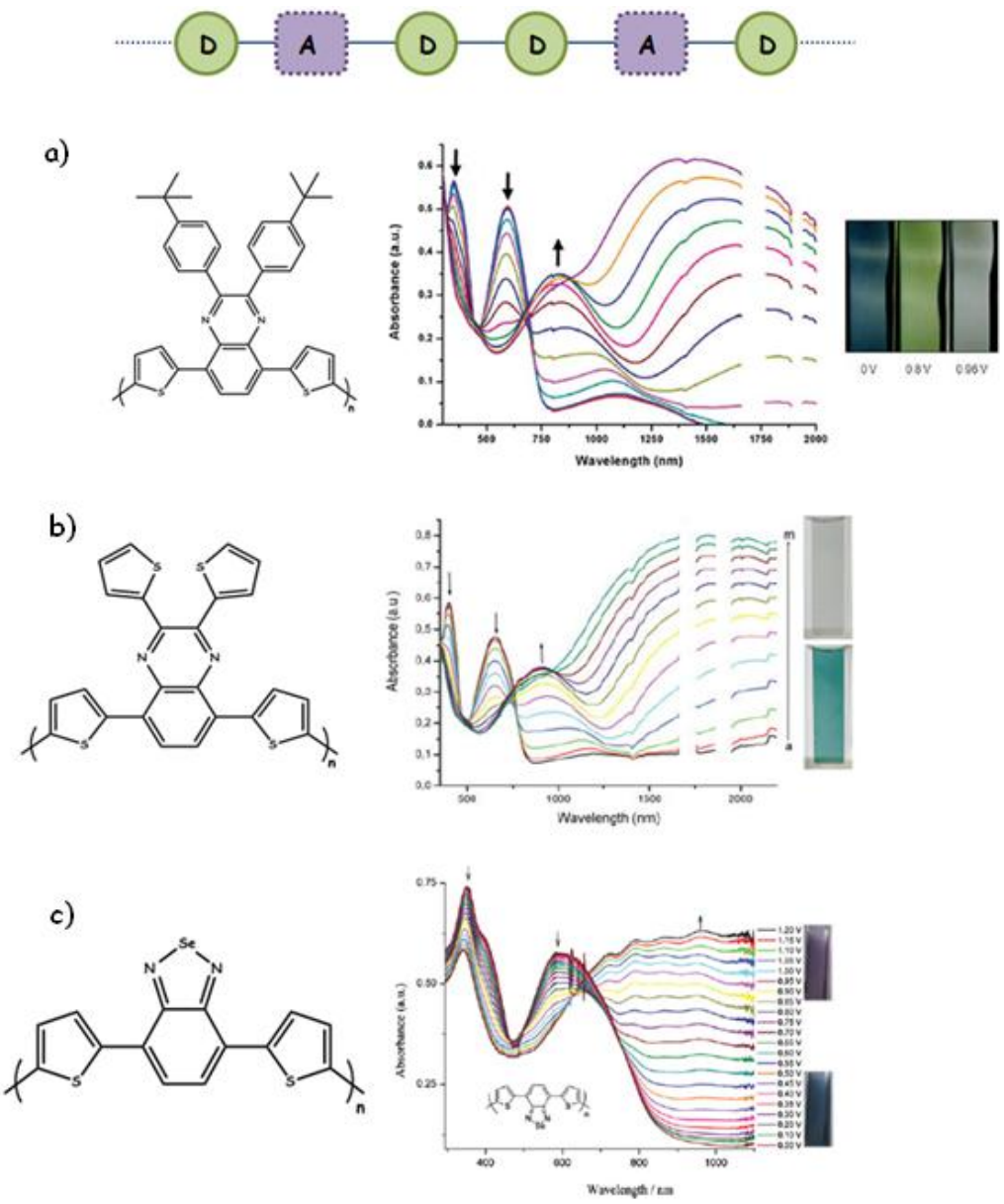

Figure 3.4 Spectroelectrochemistry and colors of D-A-D polymers with the additional acceptor units

On the other hand, BTz and thiophene bearing polymers are red in their neutral states with λ_{max} at ca. 500 nm (Figure 3.5). 2-Alkylbenzotriazoles were incorporated as both red color providing segments and the solubilizing

units to the thiophene. In Figure 3.5, the maximum absorption of PTBT where π-π* transitions occurs is seen as 503 nm [19]. PTBT becomes dark red colored in its neutral form. With oxidation, the formation of polaron bands intensifies, while the absorption maximum depletes. Unlike the other examples given above, the polaron bands lies at visible region here leads to the formation of several distinct colors. Herewith, brown color, black color and green color were formed by simultaneous absorption and blue color was achieved, respectively.

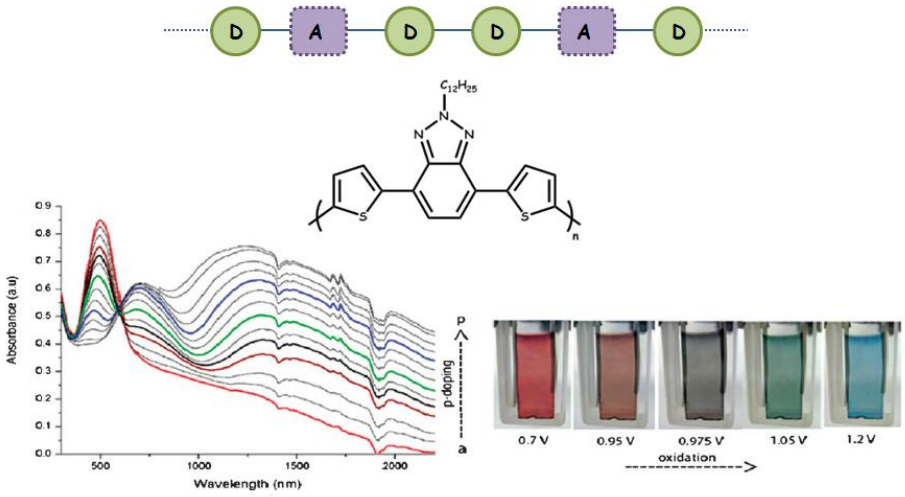

Figure 3.5 Spectroelectrochemistry ad colors of PTBT

For this study, by incorporation of neutral state red and green colored segments production of neutral state black colored copolymers were aimed. To observe the spectral behavior of the polymers in situ UV-vis-NIR spectra were taken accompanied with applied potential. Initially, neutral copolymer films were spray coated from 5mg/mL solution in chloroform. The absorbance changes were noted as the potential was gradually increased between 0.0 V and 1.5 V in 0.1 M $TBAPF_6$/ ACN (Figure 3.7). As seen in Figure 3.6, all copolymers have broad absorptions in the entire visible region. Compared to CoP1 and CoP3, CoP2 revealed a more homogenous absorption in visible region (Figure 3.6). Thus the color of the CoP2 film was black in its neutral

state. Lower energy absorption maxima of CoP2 yielded the lowest optical band gap as 1.48 eV and for CoP1:1.72 eV and CoP3:1.55 eV. Due to dominant absorbance at 600 nm, CoP3 was blue; whereas strong and blue shifted absorption resulted in purple color in neutral state for CoP1. However, since visible absorption of the films did not diminish completely upon applied potentials, oxidized forms of copolymer films revealed transmissive gray color. Thus, combination of benzoquinoxaline or benzoselenadiazole and benzotriazole with thiophene allows different segments on the same polymer chain which ended up in the absorption of all visible light.

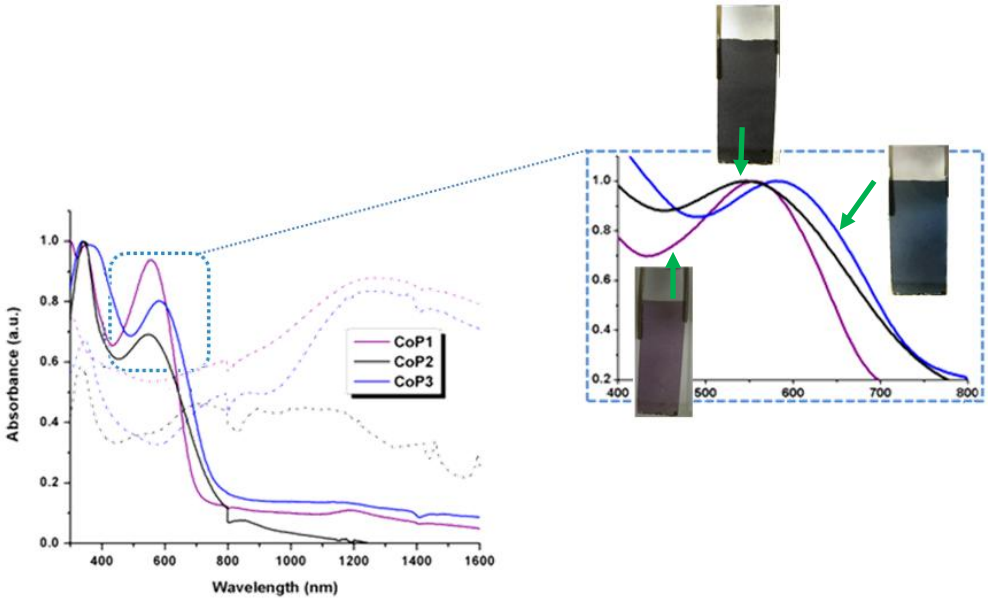

Figure 3.6 Normalized visible absorbance and neutral state colors for copolymers

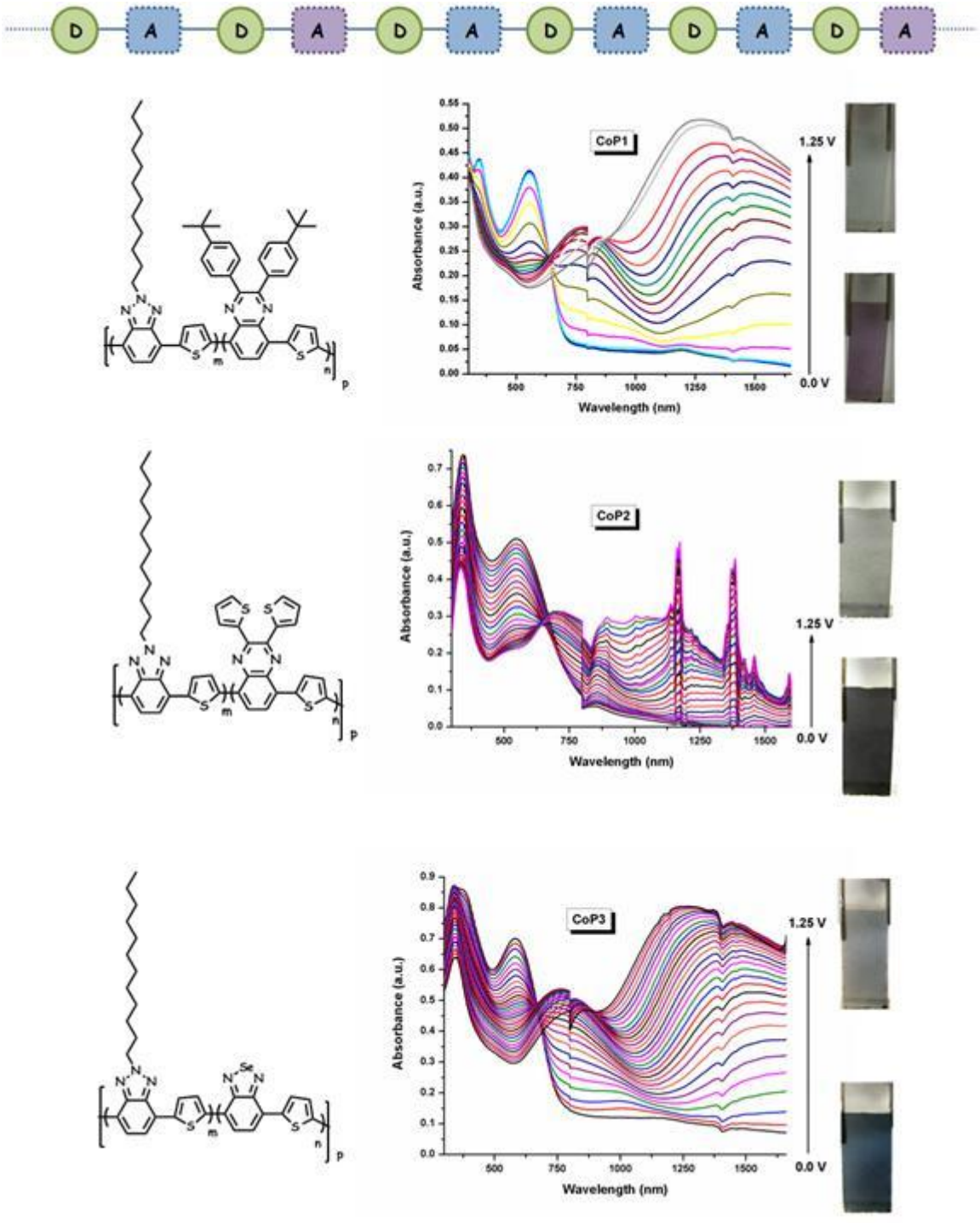

Figure 3.7 Spectroelectrochemistry of copolymer films in 0.1 M $TBAPF_6$/ ACN solution between 0.0 V and 1.25 V within 0.1 V intervals for CoP1 and 0.05 V for CoP2 and CoP3

3.3 Kinetic Studies of Random Copolymers

Switching tests were performed to monitor the percent transmittance changes as a function of time and to determine the switching times of the polymers at the wavelength (600 nm) where human eye is highly sensitive (human eye is the most sensitive at 555 nm) [68], by stepping potentials repeatedly between their fully neutral and oxidized states within 5 s time intervals. Optical contrast changes of random copolymers between their neutral and fully oxidized states between 0.0 V and 1.2 V were investigated (Figure 3.8). Under these conditions, CoP2 showed an optical contrast of 23 %. Time required for polymers to switch between their neutral and oxidized states, switching times, were defined at 95 % contrast value since human eye is sensitive up to 95 % of the full contrast. Switching times for polymers were found as 1.2 s for CoP1, 0.7 s for CoP2 and 1.0 s for CoP3. Among all, CoP2 exhibited shortest switching times as well as highest optical contrast values. For NIR region around 1200 nm, copolymers showed optical contrast as CoP1: 26% , CoP2 : 66% and CoP3: 48%.

3.4 Comparison of Alternating BTz-Th Copolymer with Random Copolymers

Due to the lack of solubility of benzoquinoxaline or benzoselenadiazole-thiophene alternating copolymers in common organic solvents, the polymers could not be spray coated on ITO surface in order to examine for their electrochemical and optical properties. Accordingly, the results were discussed only with the BTz and thiophene containing alternating copolymer which possesses a segment (BTz-Th) in all random copolymers [69].

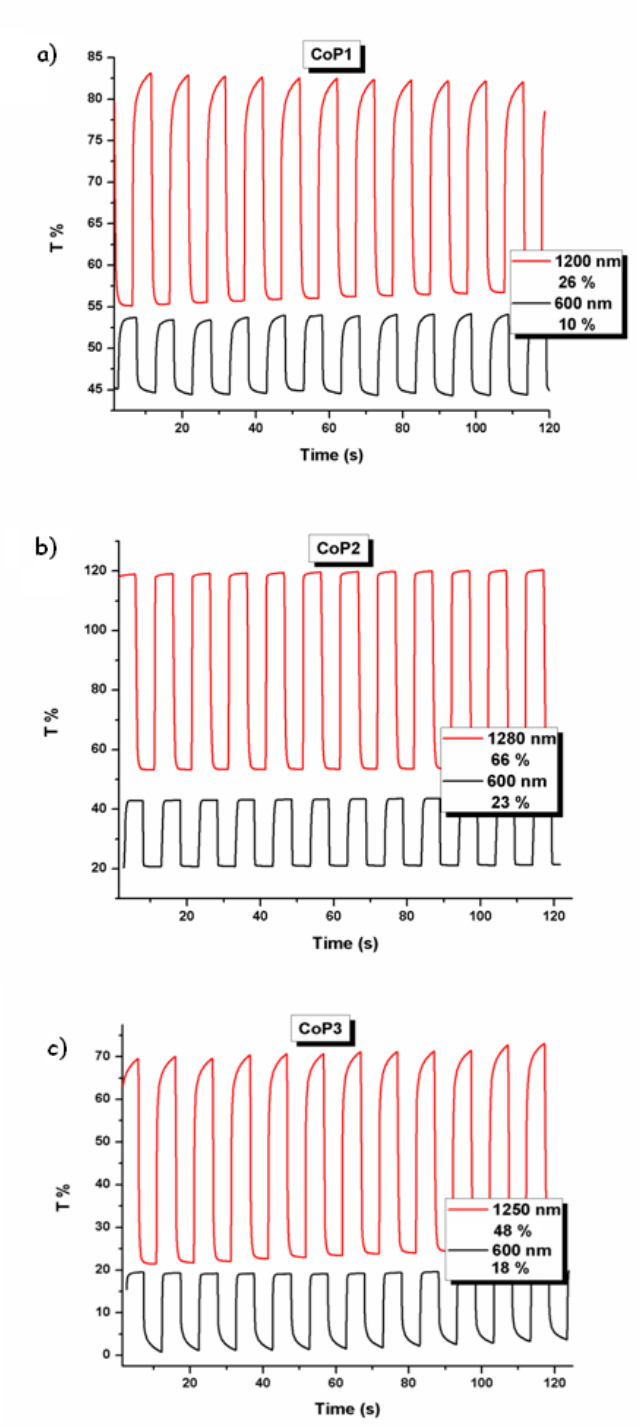

Figure 3.8 Optical contrast changes of random copolymer when switched between their neutral and fully oxidized states (0.0 V and 1.2 V) a) CoP1 film at 600 and 1200 nm, b) CoP2 film at 600 and 1280 nm, c) CoP3 film at 600 and 1250 nm

Among copolymers synthesized via Stille coupling to give random and alternating copolymer of BTz and thiophene (PTBTDA12), CoP1 has the lowest oxidation potential owing to the contribution of *tert*butylphenyl groups to the electron density of polymer. In CoP1, the polymer chain is more electron rich compare to others. From this point of view, the only variable for these copolymers is the additional acceptor units. Therefore, the difference in optical and electronic properties can be compared by focusing on the structures of additional acceptor units (Table 3.1). Due to its strong electron deficient nature, benzoselenadiazole containing random copolymer is hard to oxidize and easy to reduce. The potential required for receiving electrons from PTBTDA12 is nearly the same as CoP2 meaning that the structures are in close range in terms of electron density on the polymer backbone. All four polymers have ambipolar nature; both p and n dopable. By means of this dual type dopability, HOMO and LUMO levels can be calculated, hence the electronic band gaps. As mentioned before, CoP1 has the most electron rich nature due to its lowest oxidation potential, and thus HOMO level of CoP1 is expected to be highest among others.

Table 3.1 Comparison of the optical and electronic properties of random copolymers with alternating copolymer of BTz and Th

	CoP1	CoP2	CoP3	PTBTDA12
E_{ox} (V)	0.85	0.98	1.23	0.96
E_{red} (V)	-1.80	-1.99	-1.77	-1.82
HOMO-LUMO	-5.22/-3.55	-5.41/-3.65	-5.63/-3.81	-5.45/-3.50
E_g^{ec} (eV)	1.67	1.76	1.82	1.93
E_g^{op}(eV)	1.72	1.48	1.55	1.73
Optical Contrast at visible at N-IR	 10% 26%	 23% 66%	 18% 48%	 20%
Switching time	1.2 s	0.7 s	1.0 s	1.4 s

As a result of this increase in HOMO level, the electronic band gap of CoP1 is the lowest. This low band gap may be originated from the highly conjugated structure of additional acceptor unit composing random copolymer 1. PTBTDA12 possesses the highest band gap both electronic and optical. The highest value in optical band gap arises from the absorption maxima of alternating copolymer at 540 nm. While calculating optical band gap, the onset wavelength value of absorption maxima is taken. For PTBTDA12, it is higher since the cyan-green region absorption occurs by creating neutral state red colored material. The line of the absorption shoulder intersects the axis at shorter wavelengths than the random copolymers which have broad absorptions at visible region. As a result of this, the optical band gap of PTBTDA12 becomes high among them. Like PTBT, due to the lying of the absorption of polaron bands in the visible region, the polymer reveals different colors in the course of oxidation (Figure 3.9).

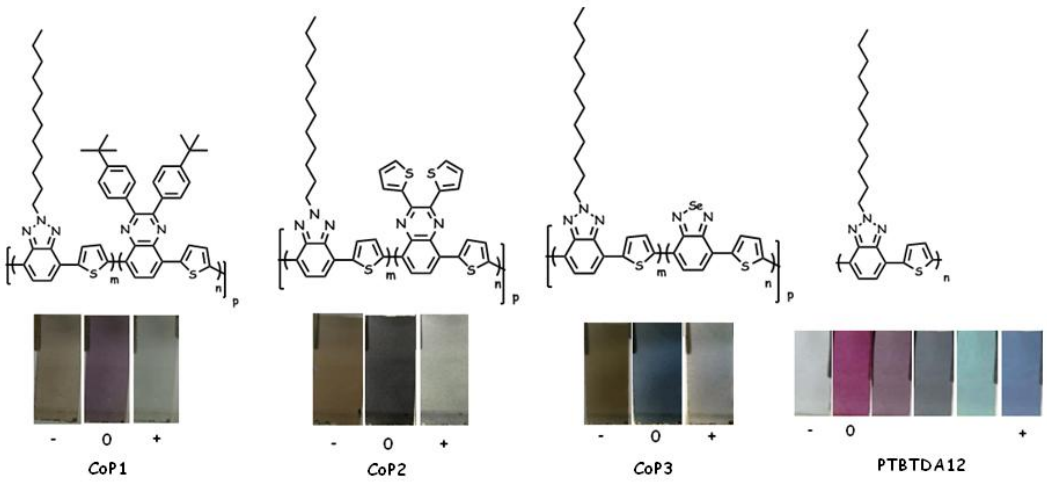

Figure 3.9 Structures and colors of copolymers upon both p and n doping

In addition to black color, green color is a mid- state. By the distinction of polaronic and neutral chain absorptions arising from the simultaneous absorptions at red and blue regions, the PTBTDA12 is colored as green. Finally, with further oxidation polymer becomes blue colored. Diversely from the alternating copolymer, random copolymers do not have multichromic nature due to the nonexistence of polaron formation in the visible region. CoP1 is purple,

CoP2 is black and CoP3 is dark blue in their neutral states. The incorporation of red and green neutral state colored materials to cover entire visible spectrum was achieved with CoP2 (Figure 3.10). During reduction of the polymer films, PTBTDA12 shows highly transparent color due to the complete depletion of neutral state absorptions. The random copolymers, on the other hand, possess orange-brown color in their reduced forms. Among all four, CoP2 shows the best kinetic features such as 23 % optical contrast at visible region with a switching time of 0.7 s.

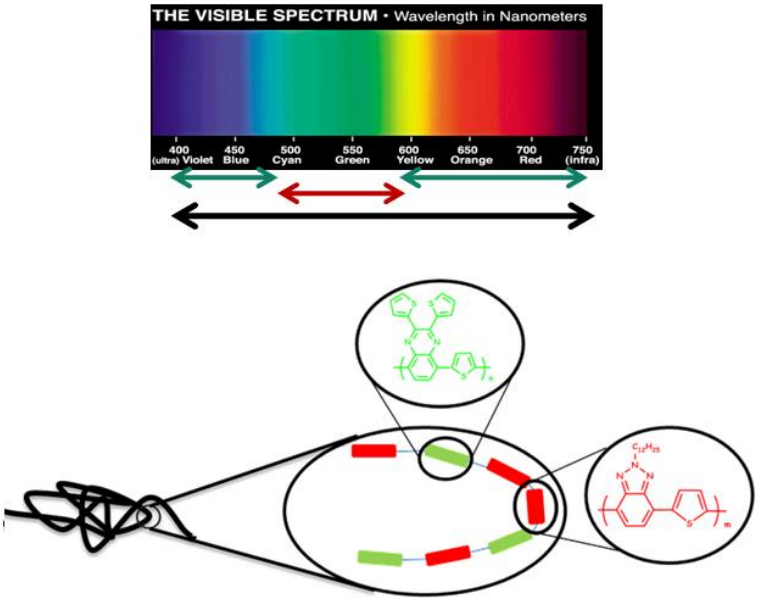

Figure 3.10 Schematic representation of the logic lies behind the formation of neutral state black colored copolymer

CHAPTER 4

CONCLUSION

Copolymerization towards obtaining full visible absorption was highlighted. Randomly distributed segments of different oligomers resulted in neutral state black copolymer. Solution processability and highly transmissive gray oxidized states make copolymers great candidates to be used in low cost flexible organic electronics. DA type benzotriazole containing copolymers were synthesized via Stille polycondensation reaction. Their potentials as full visible absorbing materials were investigated. Copolymers designed to reveal a mixed colors of different oligomer segments. To achieve full visible absorption, green (400 nm and 700 nm) and red (500 nm) materials were combined. 2-Alkylbenzotriazoles were incorporated as both red color providing segments and the solubilizing units. Among all the three, dithienylbenzoquinoxaline containing copolymer CoP2 absorbs almost all visible light and reveals a black color in its neutral state. Additionally highly transmissive state for CoP2 makes it a great candidate for smart windows applications with 23 % optical contrast and 0.7 s switching time. Highlighted results showed that these polymers can be used in non-emissive electrochromic applications as well as different organic electronic applications where neutral state visible absorbance is of importance. Kinetic properties such as optical contrasts (10 % , 23 % and 18 % at 600 nm) and switching times (1.2 s, 0.7 s, and 1 s) make them potential materials to be used in devices. Nevertheless, these polymers need further investigation for their different structural derivatives for applications in solar cells and electrochromic display devices.

This study was published in the journal of Chemical Communications in February, 2011 [70].

REFERENCES

[1] P. M. Beaujuge and J. R. Reynolds, *Chem. Rev*., **2010**, 110, 268.

[2] S. Beaupre, P. T. Boudreault and M. Leclerc, *Adv. Mater.,* **2010**, 22, E6.

[3] H. Letheby, *J. Chem. Soc.*, **1862**, 15, 161.

[4][a] H. Shirakawa, E. J. Louis, A. G. MacDiarmid, C. K. Chiang, A. J. Heeger, *J. Chem. Soc., Chem. Commun.*, **1977**, 578., [b] C. K. Chiang, C. R. Fischer, Y. W. Park, A. J. Heeger, H. Shirakawa, E. J. Louis, S. C. Gau, A. G. MacDiarmid, *Phys. Rev. Lett.*, **1977**, 39,1098.

[5] A. G. MacDiarmid, *Angew. Chem. Int. Ed.*, **2001**, 40, 2581.

[6] K. E. Ziemelis, A. T. Hussain, D. D. C. Bradley, R. H. Friend, J. Rilhe, G. Wegner, *Phys. Rev. Lett.*, **1991**, 66, 2231.

[7] P. J. Nigrey, A. G. MacDiarmid, A. J. Heeger, *J. Chem. Soc. Chem. Commun.*,**1979**, 594.

[8] J. J. Apperloo, R. A. J. Janssen, M. M. Nielsen, K. Bechgaard, *Adv. Mater.*, **2000**,12, 1594.

[9] R. Hoffmann, *Angew. Chem Int Ed*., **1987**, 26, 846.

[10] K. Shimamura, F.E. Karasz, J.A.Hirsch, J.C. Chien*, Macromol. Chem. Rapid Commun.*, **1981**, 2, 443.

[11][a] F. Wudl, M. Kobayashi, A. J. Heeger, *J. Org. Chem.*, **1984**, 49, 3382., [b] J. Roncali, *J. Mater. Chem.*, **1999**, 9, 1875.

[12][a] J. Roncali, *Chem. Rev.*, **1997**, 97, 173., [b] J. Roncali, *Macromol. Rapid Commun.*, **2007**, 28, 1761.

[13] H. A. M. Mullekom, J.A.J.M. Vekemans, E.E. Havinga and E.W. Meijer. *Mater. Sci. Eng.* ,**2001**,R32,1.

[14] U. Salzner, M.E. Kose, *J. Phys. Chem. B.*, **2002**, 106, 9221.

[15] C.A. Thomas, K. Zong, K.A. Abboud, P.J. Steel and J.R. Reynolds, *J Am Chem Soc*., **2004**, 126, 50, 16440.

[16][a] T. Yasuda, T. Imase, T. Yamamoto, *Macromolecules*. **2005**, 38, 7378., [b] T. Yamamoto, K. Sugiyama, T. Kanbara, H. Hayashi, H. Etori, *Macromol. Chem. Phys.* **1998**, 199, 1807.

[17] [a] T. Kanbara, T. Yamamoto*, Chem. Lett*, **1993**, 22, 419. [b] Y. Tsubata, T. Suzuki, T. Miyashi and Y. Yamashita, *J. Org. Chem*. **1992**, 57, 6749.

[18] A. Tanimoto, T. Yamamoto, *Macromolecules*, **2006**, 39, 3546.

[19] A. Balan, G. Gunbas, A. Durmus and L. Toppare, *Chem. Mater.*, **2008**, 20, 7510.

[20] A. Balan, D. Baran, G. Gunbas, A. Durmus, F. Ozyurt and L. Toppare, *Chem. Commun*., **2009**, 6768.

[21] D. Baran, A. Balan, B. M. Esteban, H. Neugebauer, N. S. Sariciftci and L. Toppare, *Macromol. Chem. Phys*., **2010**, 211, 2602.

[22] M. Icli, M. Pamuk, F. Algi, A. M. Onal and A. Cihaner, *Chem. Mater.*, **2010**, 22, 4034.

[23] N. Akbasoglu, A. Balan, D. Baran, A. Cirpan and L. Toppare, *J. Polym. Sci., Part A: Polym. Chem.*, **2010**, 48, 5603.

[24] D. Baran, A. Balan, S. Celebi, B. M. Esteban, H. Neugebauer, N. S. Sariciftci and L. Toppare, *Chem. Mater.*, **2010**, 22, 2978.

[25] G. Cetin, A. Balan, G. Gunbas, A. Durmus and L. Toppare, *Org. Electron.*,**2009**,10, 34.

[26] P. R. Somani, S. Radhakrishnan, *Mater. Chem. and Phys.*, **2002**, 77, 117.

[27] R. J. Mortimer, *Electrochimica Acta*, **1999**, 44, 2971.

[28] C. L. Gaupp, J. R. Reynolds, *Macromolecules*, **2003**, 36, 6305.

[29] N. M. Rowley, R. J. Mortimer, *Science Progress* , **2002**, 85 ,243.

[30] J.H. Burroughes, D.D.C. Bradley, A.R Brown, R.N Marks, K. Mackay, R.H Friend, P.L Burn, A.B Holmes, *Nature*, **1990**, 347, 539.

[31] F. Babudri, G. M. Farinola, F. Naso, R. Ragni, *Chem. Commun.*, **2007**, 1003.

[32] A. A. Argun, PhD Thesis, University of Florida, **2004**.

[33] R. E. Gill, G.G. Malliaras, J. Wildeman, G. Hadziioannou, *Adv. Mater.*, **1994**,6, 132.

[34] R. M. Walczak and J. R. Reynolds, *Adv. Mater.*, **2006**, 18, 1121.

[35] A. L. Dyer, M. R. Craig, J. E. Babiarz, K. Kiyak and J. R. Reynolds, *Macromolecules*, **2010**, 43, 4460.

[36] A. Berlin, G. Zotti, S. Zecchin, G. Schiavon, B. Vercelli and A. Zanelli, *Chem. Mater.*, **2004**, 16, 3667.

[37] G. Sonmez, C. K. F. Shen, Y. Rubin and F. Wudl, *Angew. Chem. Int. Ed.*, **2004**, 43, 1498.

[38] A. Durmus, G. E. Gunbas, P. Camurlu and L. Toppare, *Chem.Commun.*, **2007**, 3246.

[39] [a] A. Durmus, G. E. Gunbas and L. Toppare, *Chem. Mater.*, **2007**, 19, 6247., [b] G. E. Gunbas, A. Durmus and L. Toppare, *Adv. Mater*., **2008**, 20, 691., [c] G. E. Gunbas, A. Durmus and L. Toppare, *Adv. Funct. Mater.*,**2008**, 18, 2026.

[40] Q. Pei, G. Zuccarello, M. Ahlskog and O. Inganas,. *Polymer.*, **1994**, 35 (7), 1347.

[41] A. Balan, D. Baran, N. S. Sariciftci and L. Toppare, *Sol. Energy Mater. Sol. Cells.*, **2010**, 94, 1797.

[42] C. M. Amb, P. M. Beaujuge and J. R. Reynolds, *Adv. Mater.*, **2010**, 22, 724.

[43] F. C. Krebs, *Nat. Mater.*, **2008**, 7, 766.

[44] S. Gunes, H. Neugebauer and N. S. Sariciftci, *Chem. Rev.*, **2007**, 107,1324.

[45] P. M. Beaujuge, S. Ellinger and J. R. Reynolds, *Nat. Mater.*, **2008**, 7, 795.

[46] P. Shi, C. M. Amb, E. P. Knott, E. J. Thompson, D. Y. Liu, J. Mei, A. L. Dyer and J. R. Reynolds, *Adv. Mater.*, **2010**, 22, 4949.

[47] M. Icli, M. Pamuk, F. Algı, A. M. Onal and A. Cihaner, *Org. Electron.*, **2010**, 11, 1255.

[48] D. Kumar, R. C. Sharma, *Eur. Polym. J.*, **1998**, 34, 1053.

[49] I. F. Perepichka, D. F. Perepichka, H. Meng, F. Wudl, *Adv. Mater.*, **2005**, 17, 2281.

[50] T. Yamamoto, K. Sanechika, A. Yamamoto, *J. Polym. Sci., Polym. Lett.* **1980,** 18, 9.

[51] J. W. P. Lin, L.P. Dudek, *J. Polym. Sci., Part A,* **1980**, 18, 2869.

[52] M. Kobayashi, J. Chen, T.C. Chung, F. Moraes, A.J. Heeger, F. Wudl, *Synth. Met.* **1984,**9,77.

[53] T. Yamamoto, A. Morita, Y. Miyazaki, T. Maruyama, H. Wakayama, Z. Zhou, Y. Nakamura, T. Kanbara, S. Sasaki, K. Kubota, *Macromolecules* **1992,** 25, 1214.

[54] R. D. McCullough, R. D. Lowe, M. Jayaraman, D. L. Anderson, *J. Org. Chem.*, **1993**, 58, 904.

[55] T.A. Chen, X. M. Wu, R. D. Rieke, *J. Am. Chem. Soc.* **1995,** 117, 233.

[56] E. A. Meijere, F. Diederich, Metal-Catalyzed Cross-Coupling Reactions, Wiley-VCH, Weinheim, **2004**, (2).

[57] Palladium-Catalyzed Cross Couplings in Organic Synthesis, The Royal Swedish Academy of Sciences, Sweden, **2010**.

[58] J. K. Stille, *Angew. Chem., Int. Ed. Engl.*, **1986**, 25, 508.

[59] J. Roncali*, Chem Rev.*, **1992**, 92, 711.

[60] [a] F. Ozyurt, E.G. Gunbas, A. Durmus and L. Toppare, *Org.Electron*., **2008**, 9, 296, [b] E.G. Gunbas, A. Durmus and L. Toppare, *Adv.Mater*., **2008**, 20, 691.

[61] H. Becker, K. Treacher, H. Spreitzer, A. Falcou, P. Stoessel, A. Buesing and A. Parham, *PCT Int. Appl*., **2003**, 020790.

[62] Y. Tsubata, T. Suzuki, T. Miyashi and Y. Yamashita, *J. Org. Chem*., **1992**, 57, 6749.

[63] X. Guo and M. D. Watson, *Org. Lett.*, **2008**, 10, 5333.

[64] E.R Kötz, H. Neff and K. Müller, *J. Electroanal. Chem,***1986**, 215, 331.

[65] M. Sendur, A. Balan, D. Baran and L. Toppare, *J. Polym. Sci. Part A: Polym. Chem.*, **2011**, 4065.

[66] Y. Arslan Udum, E. Yıldız, G. Gunbas and L. Toppare, *J. Polym. Sci. Part A: Polym. Chem.*, **2008**, 3723.

[67] A. Cihaner and F. Algı, *Adv. Funct. Mater.*, **2008**, 3583.

[68] S. W. Lockley, G. C. Brainard, C.A. Czeisler, *J. Clin. Endocrinol. Metab.,* **2003**, 88, 4502.

[69] A. Balan, D. Baran and L. Toppare, *J. Mater. Chem.*, **2010**, 20, 9861.

[70] G. Oktem, A. Balan, D. Baran and L. Toppare, *Chem. Commun.,* **2011**, 47, 3933.

APPENDIX A

NMR DATA

NMR spectra were recorded on a Bruker Spectrospin Avance DPX-400 Spectrometer. Chemical shifts δ are reported in ppm relative to $CHCl_3$ (^1H: δ=7.27), $CDCl_3$ (^{13}C: δ=77.0) and CCl_4 (^{13}C: δ=96.4) as internal standards.

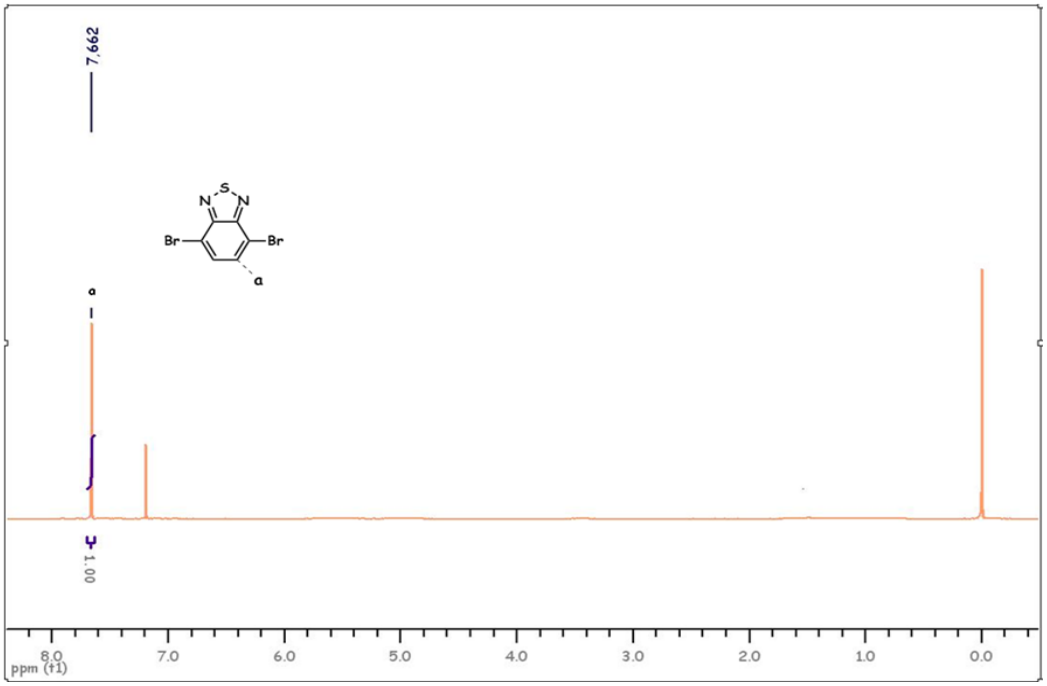

Figure A.1 ^1H-NMR spectrum of 4,7-dibromobenzothiadiazole (1)

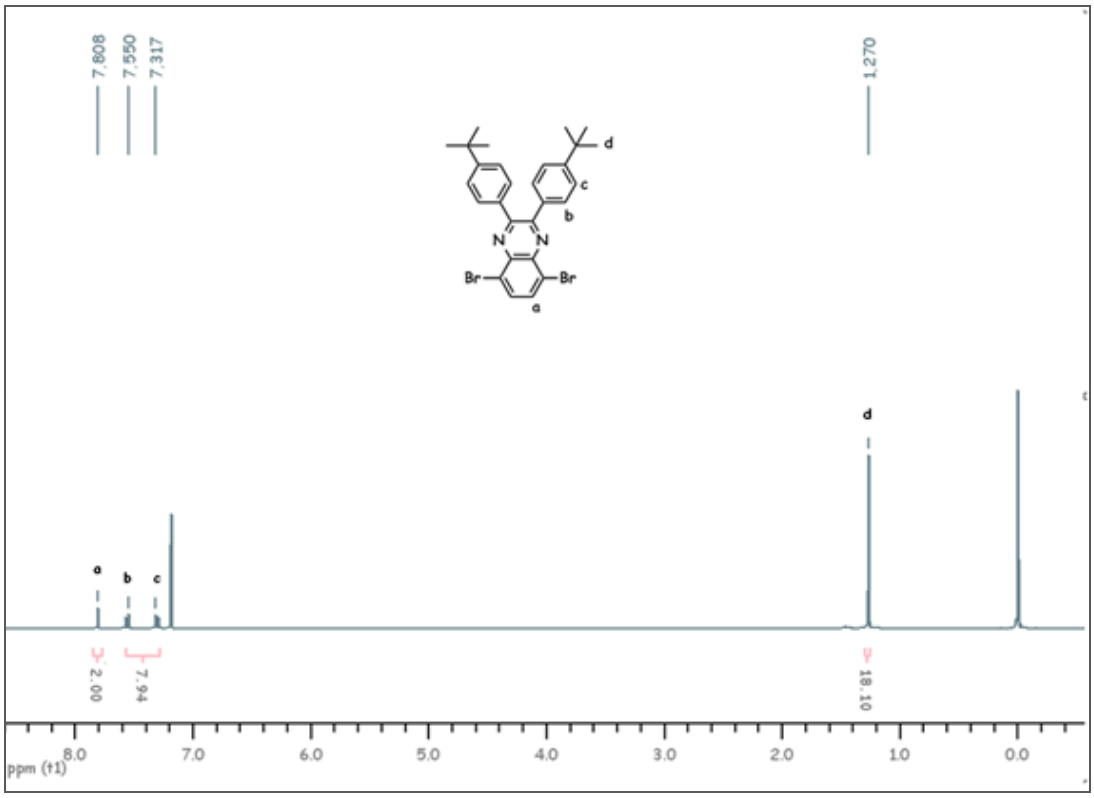

Figure A.2 ^{1}H-NMR spectrum of 5,8-dibromo-2,3-bis(4-*tert*-butylphenyl)quinoxaline (3)

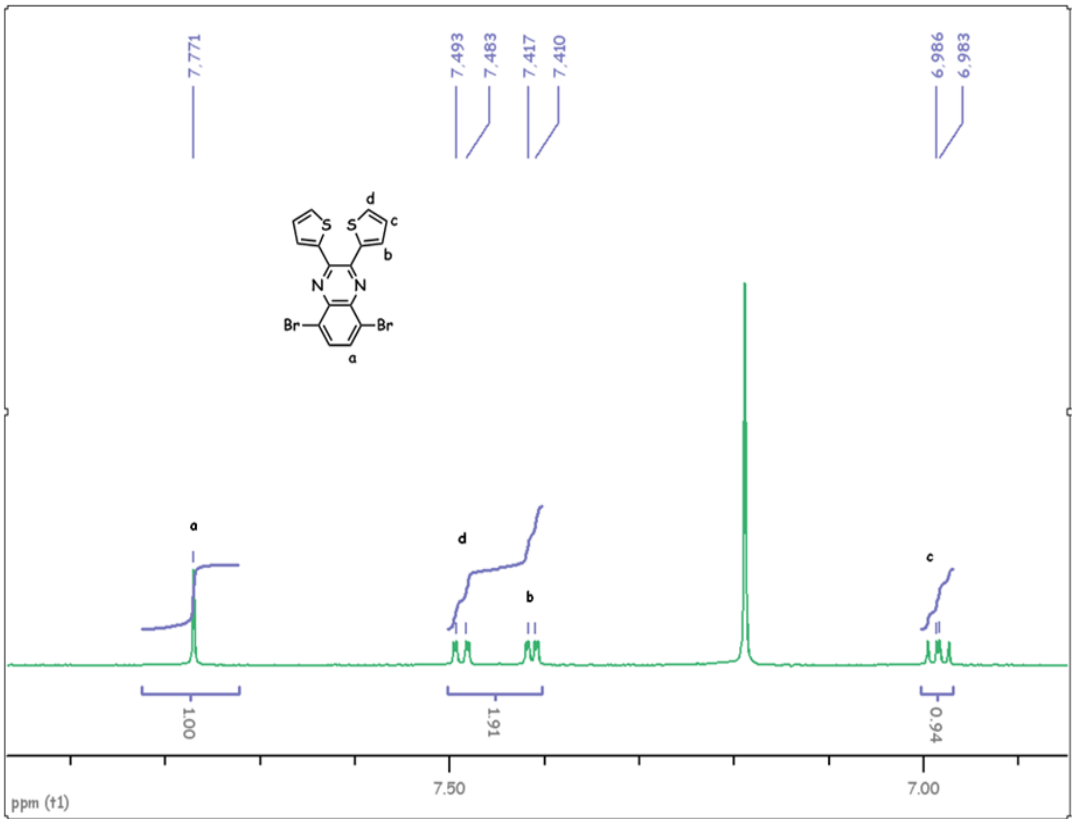

Figure A.3 ^{1}H-NMR spectrum of 5,8-dibromo-2,3-di(thiophen-2-yl)quinoxaline (4)

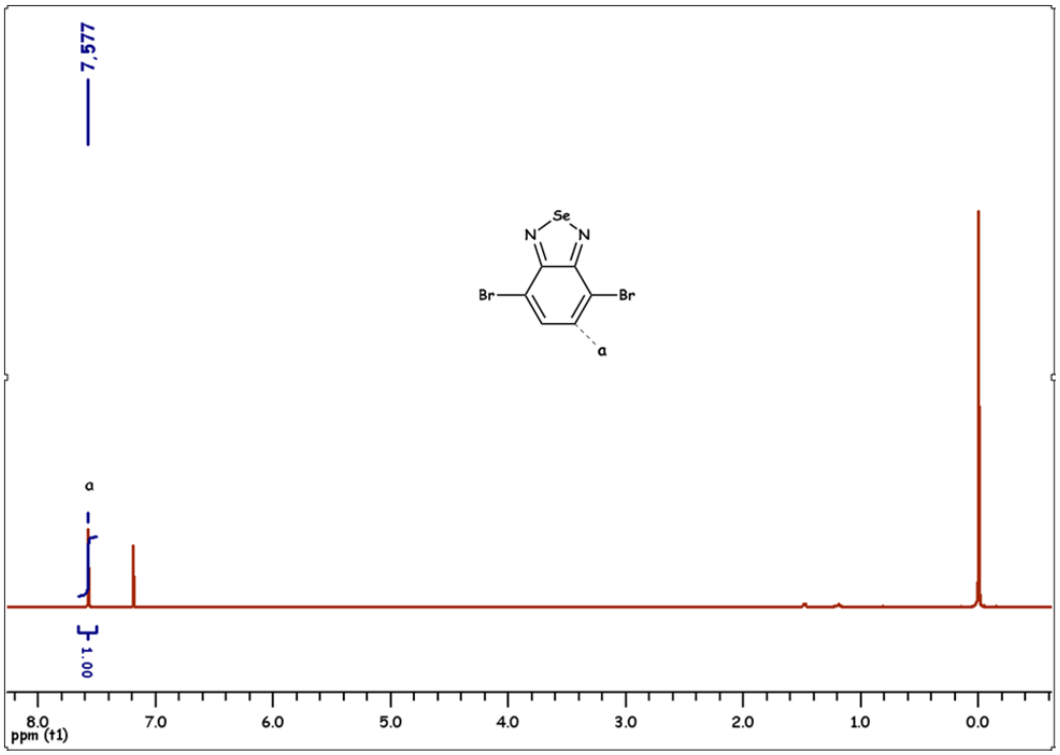

Figure A.4 ^{1}H-NMR spectrum of 4,7-dibromobenzo[c][1,2,5] selenadiazole (5)

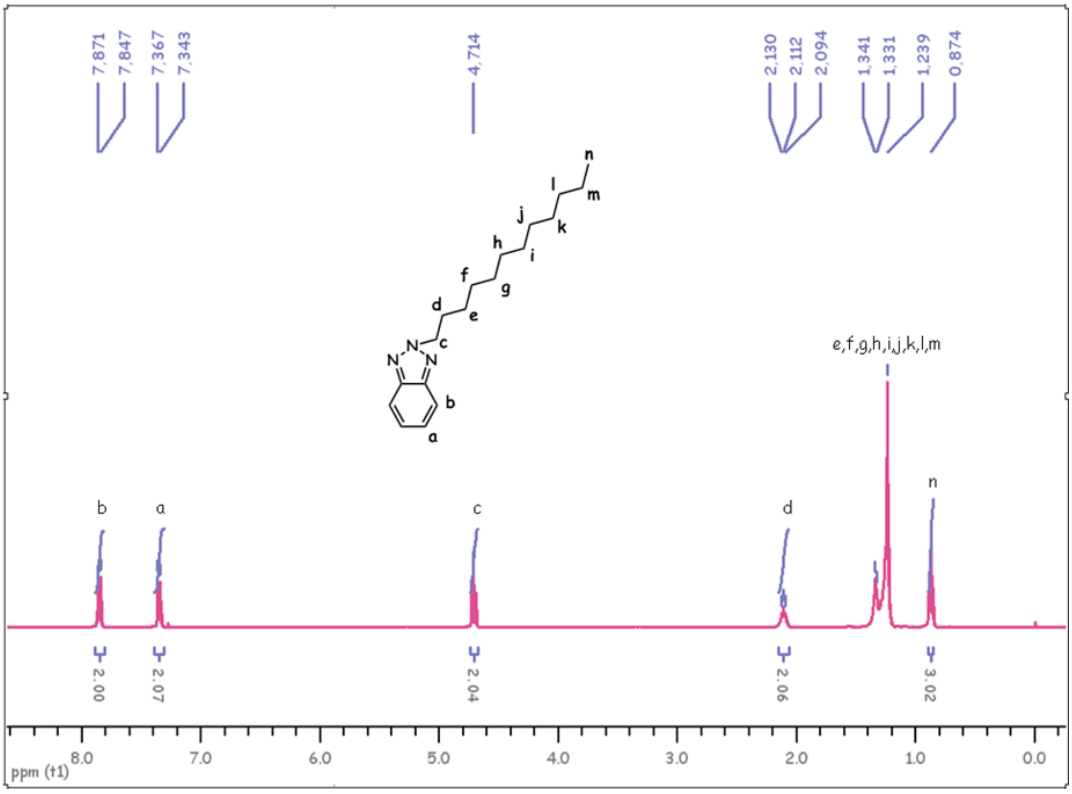

Figure A.5 ^{1}H-NMR spectrum of 2-dodecyl-2H-benzo[d][1,2,3]triazole (6)

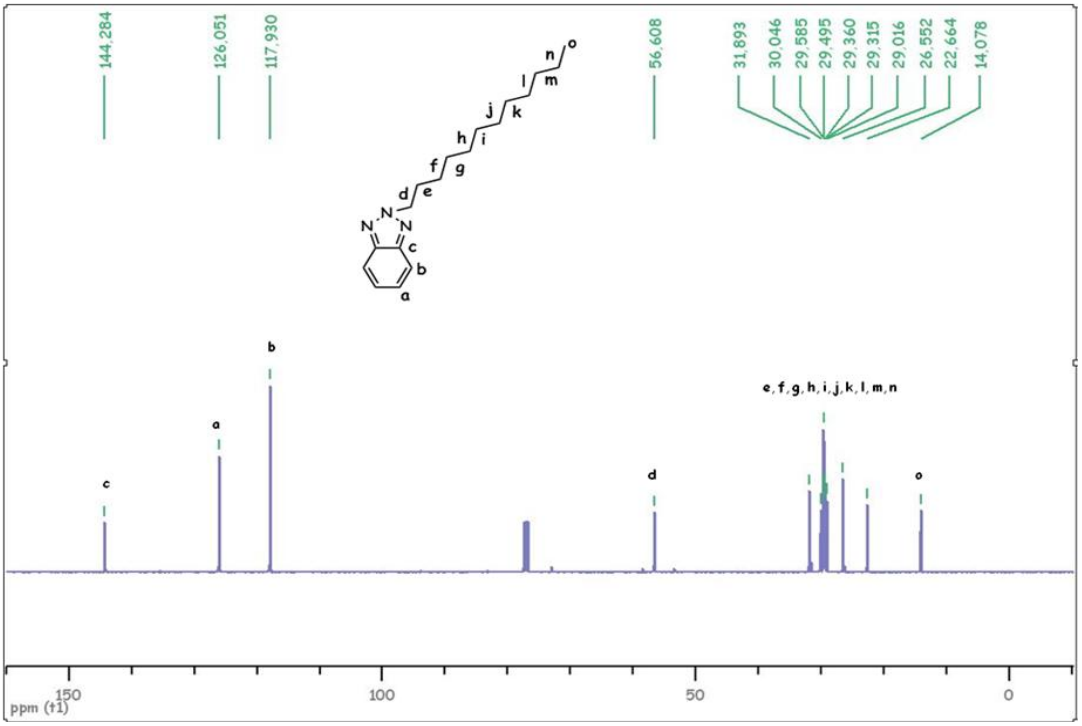

Figure A.6 ^{13}C-NMR spectrum of 2-dodecyl-2H-benzo[d][1,2,3]triazole (6)

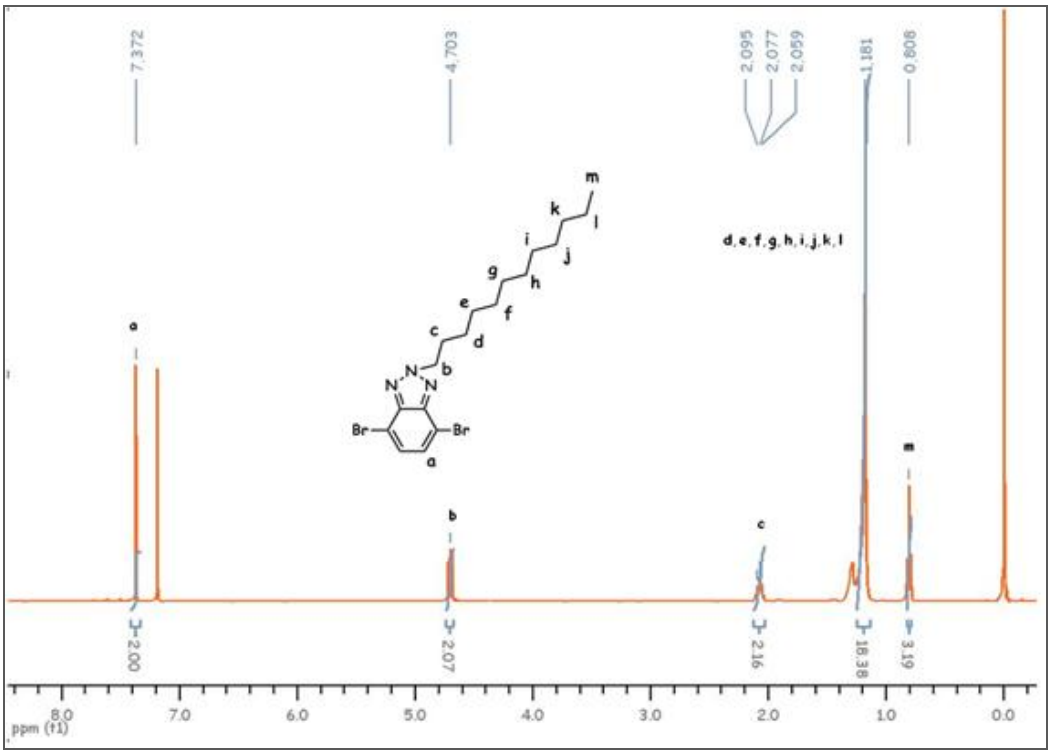

Figure A.7 ^{1}H-NMR spectrum of 4,7-dibromo-2-dodecyl-2H-benzo[d][1,2,3]triazole (7)

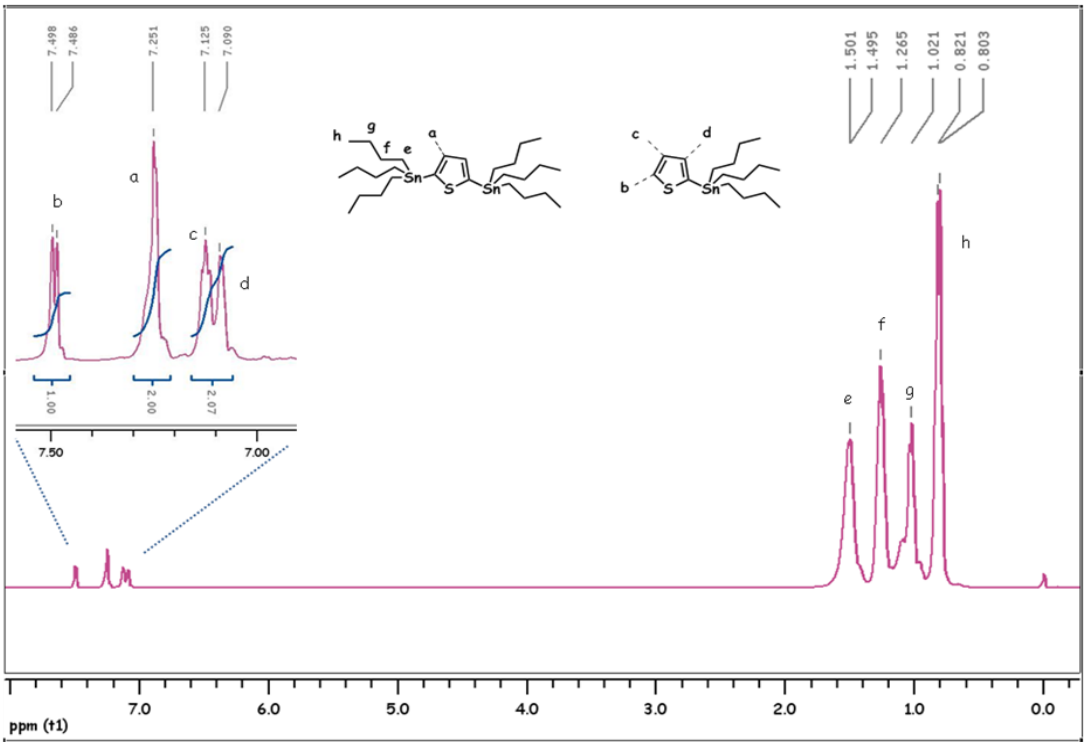

Figure A.8 ^{1}H-NMR spectrum of 2,5-bis(tributylstannyl)thiophene (8)

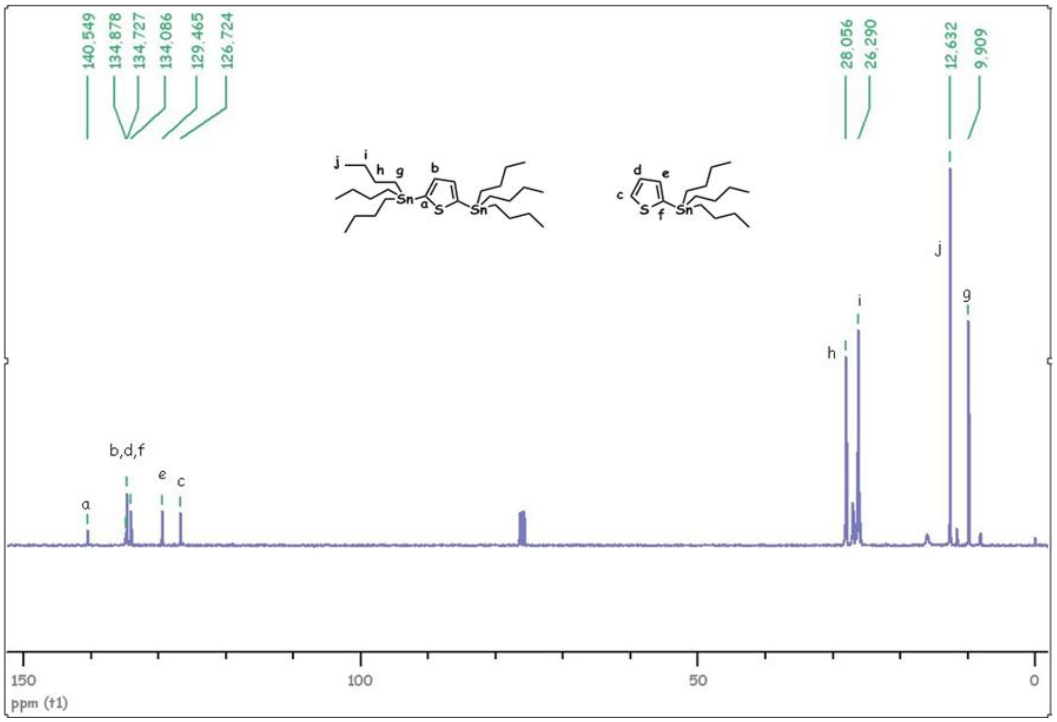

Figure A.9 ^{13}C-NMR spectrum of 2,5-bis(tributylstannyl)thiophene (8)

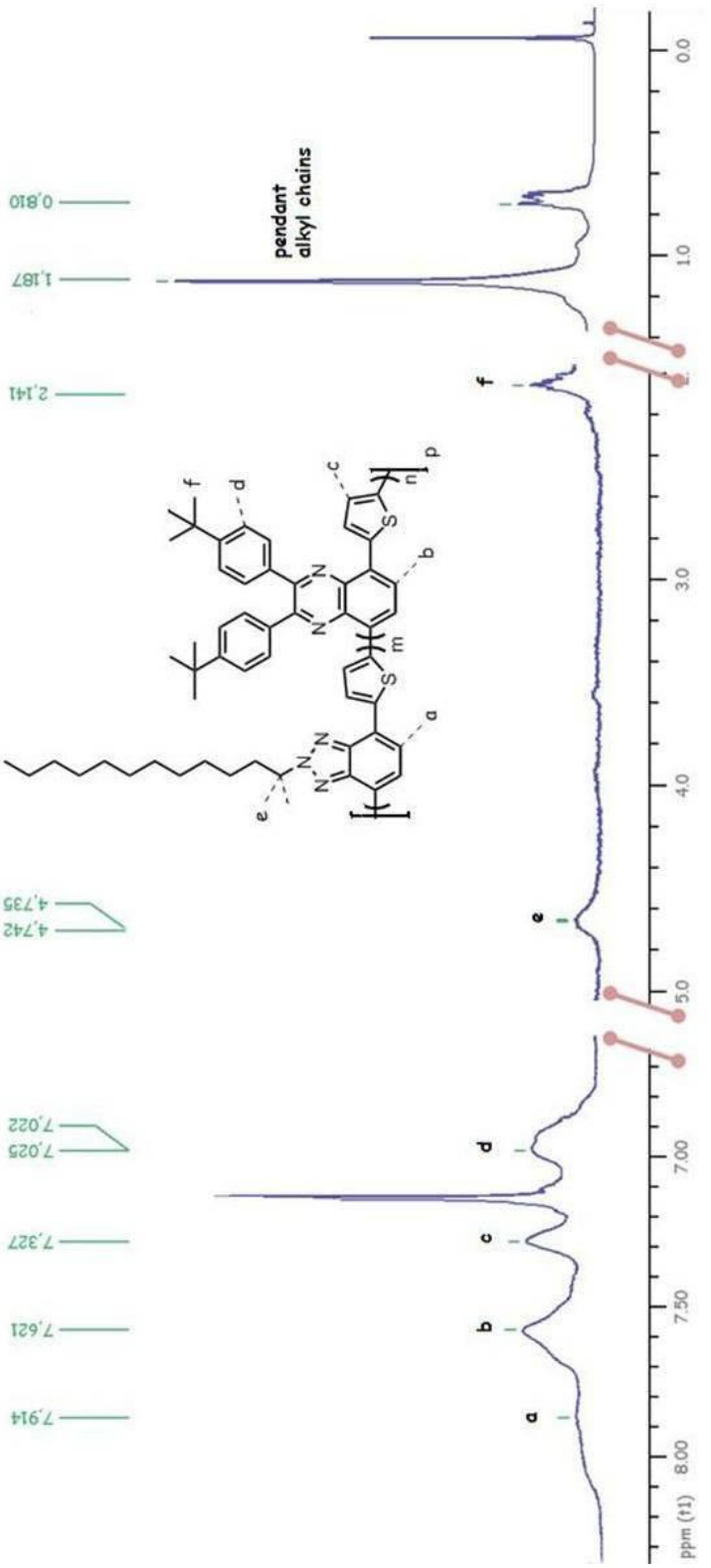

Figure A.10 ^{1}H-NMR spectrum of Copolymer **1**

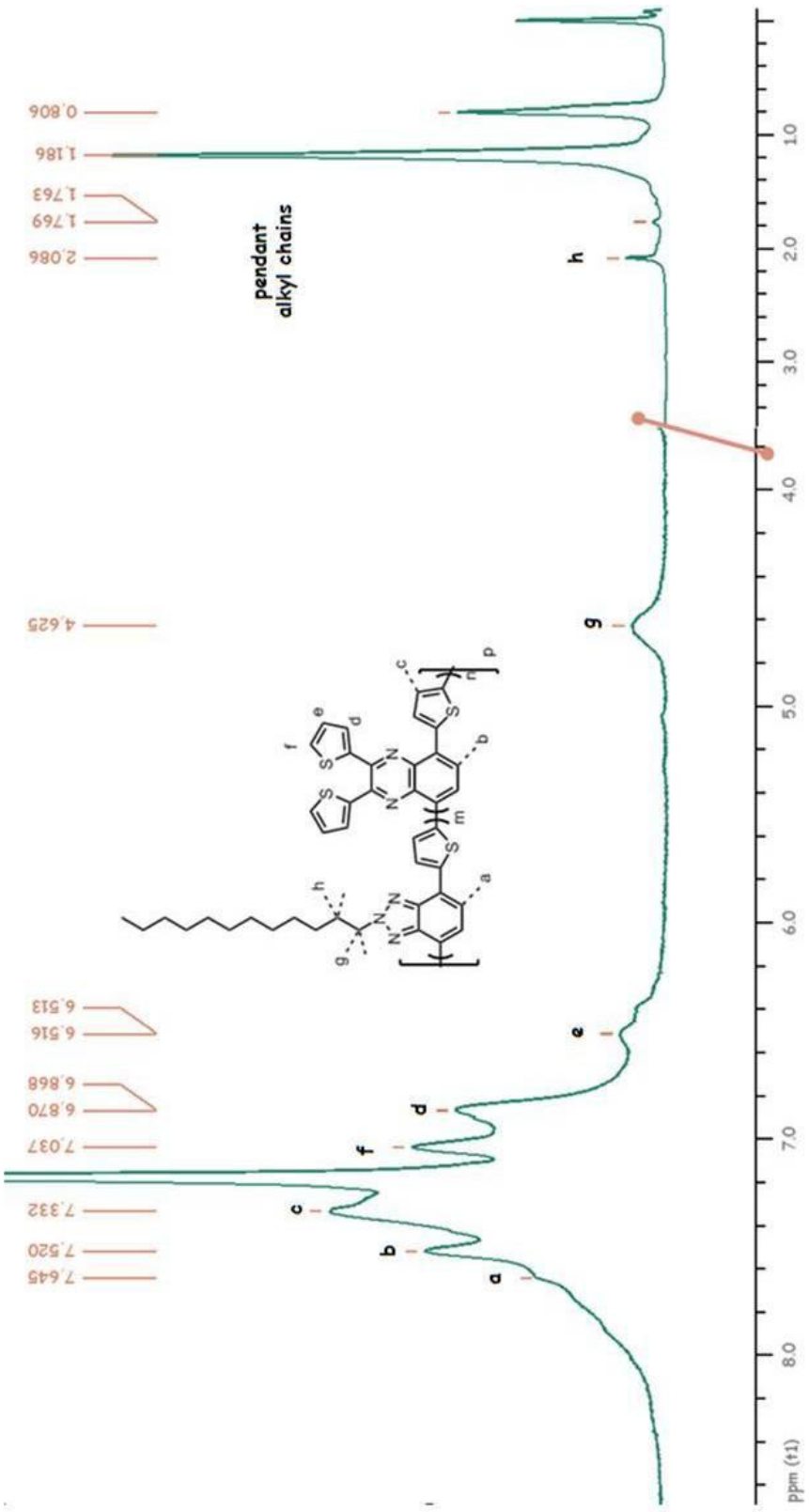

Figure A.11 ^{1}H-NMR spectrum of Copolymer **2**

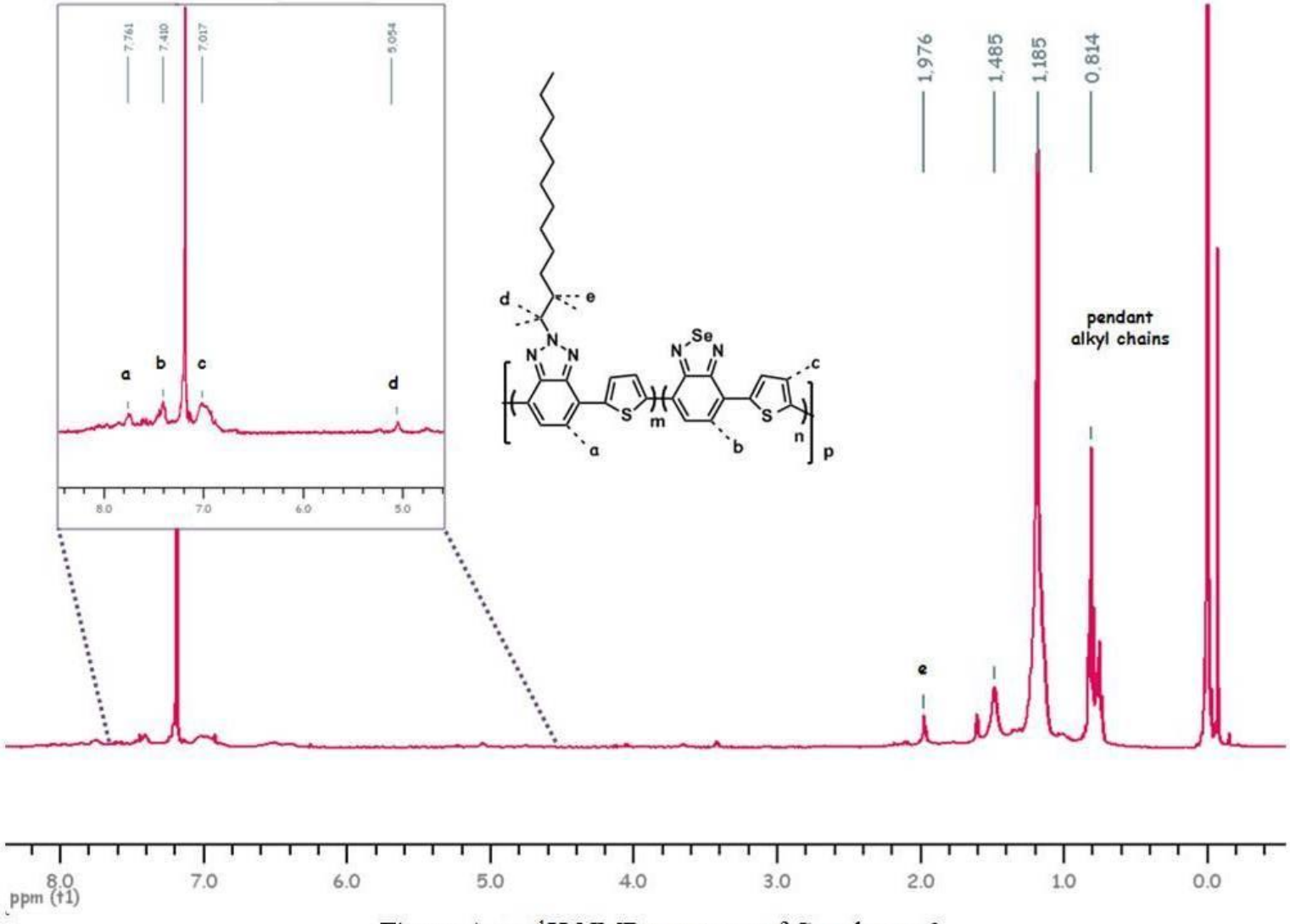

Figure A.12 ^{1}H-NMR spectrum of Copolymer **3**